



Tempus



MINISTRY OF EDUCATION AND SCIENCE OF RUSSIA  
RUSSIAN STATE HYDROMETEOROLOGICAL UNIVERSITY

*E. KOCHETKOVA, I. KOZLOV  
I. DAILIDIENĖ, K. SMIRNOV*

# REMOTE SENSING FOR OCEANOGRAPHIC APPLICATIONS

**Textbook**



Saint-Petersburg  
2013

UDK [629.782:551.46] (075.8)

BBK 26.82

K 31

Kochetkova E., Kozlov I., Dailidienė I., Smirnov K. Remote Sensing for Oceanographic Applications. Textbook. - SPb, RSHU, 2013 - 82 c.

**ISBN 978-5-86813-375-6**

*Editor Bertrand Chapron*

This textbook is intended to provide a brief reference material for the course on remote sensing of marine environment for master level students and undergraduates of senior courses. It contains general information on principles of remote sensing techniques and the variety of observations made available by spaceborne instruments. More detailed information is given on the data processing and oceanographic applications. The second part of the book offers several practical assignments to be used within the course under supervision and was specially designed to assist during the course at the Russian State Hydrometeorological University.

*This textbook is published within the framework of the project TEMPUS eMaris, funded with support of the European Commission; and also this publication was supported by the Mega-Grant of the Russian Federation Government under Grant 11.G34.31.0078, to support scientific research under the supervision of leading scientist at Russian State Hydrometeorological University.*

**ISBN 978-5-86813-375-6**

© Kochetkova E., Kozlov I., Dailidienė I.,  
Smirnov K., 2013

© Russian State Hydrometeorological  
University, (RSHU), 2013

## PREFACE

Started with early photographic cameras installed on the hot air balloons at the end of 19-th century and followed by motion cameras at the beginning of the 20-th century captures of the Earth surface appeared to provide public entertainment at first. Later those captures served for military applications reconnaissance during the war and peaked in the middle of the 20-th century as a spyware during the Cold War. The photographs taken from the aircrafts were afterwards recognized as sufficient information source for cartographers and researchers. Remote sensing approach has been exercised for several decades now as a way of receiving data from distant regions where observations are very complicated to organize as well as costly. The advantage of relatively cheap and fast way to obtain snapshots of the surface was appreciated by scientists and military administration; therefore remote sensing developed as rapidly as technologies of scanning, capturing, emitting and receiving equipment. In the mid of 20-th century oceanographic applications mainly were presented by images of ice conditions, wave studies and coastal processes definition and assessment. Around 1950s the infrared part of the spectrum was started to be used for non-military applications.

In the second half of the 20-th century the possibility of spaceborne observations has announced a new era of global scale studies. Research on oceans, continents, atmosphere and climate received reinforcement in data and information processing for civil, scientific and military needs. Data reading and transformation of scanner images have stimulated development technologies of image processing, data storage and transmitting.

Modern day formats of storage, transformation and sharing of the remote sensing data provides possibility for thousands of scientists and engineers to find new ways for studies of features that could have never been found, observed or studied before. Due to this a lot of materials are published on many aspects of the remote sensing. There are online, soft and hard cover books, movies, interactive boards and websites, and courses at colleges and universities. Still the demand for another book or information source is yet high. That is because of the numerous and various interpretations and applications the remote sensing has in modern civil, military and scientific field. This book is another transcription of principles and technologies of gaining and processing of data, focused on oceanographic use. The authors hope that the readers would benefit from the throughout information and practical approach to the remote sensing for oceanography employed in this book. The theoretical part of this book is based

on the wonderful set of two books «Discovering the Ocean from Space» and «Measuring the Oceans from Space » written by I. S. Robinson.

The textbook was published in the framework of the TEMPUS eMaris project funded with support of the European Commission; and supported by the Mega-Grant of the Russian Federation Government under Grant 11.G34.31.0078, to support scientific research under the supervision of leading scientist at Russian State Hydrometeorological University.

# PART I THEORY

## Introduction

Nowadays there are many marine-oriented satellites on the orbit providing vast amount of ready-to-use geophysical products for variety of oceanographic applications. Fig. 1 shows a basic scheme of oceanographic information retrieval from aboard the satellite sensor typically located hundreds (for polar-orbiting satellites) or thousands of kilometers (for geostationary satellites) from the sea surface.

An electromagnetic signal of a particular kind leaves the sea carrying information about one of the primary observable quantities which are the color, the radiant temperature, the roughness, and the height of the sea. This signal must pass through the atmosphere where it may be changed, and where noise may be added to it, before it is received by the sensor which detects particular properties of the radiation and converts each measurement into a digital signal to be coded and sent to the ground. The sensor geometry restricts each individual observation to a particular instantaneous field of view (IFOV).

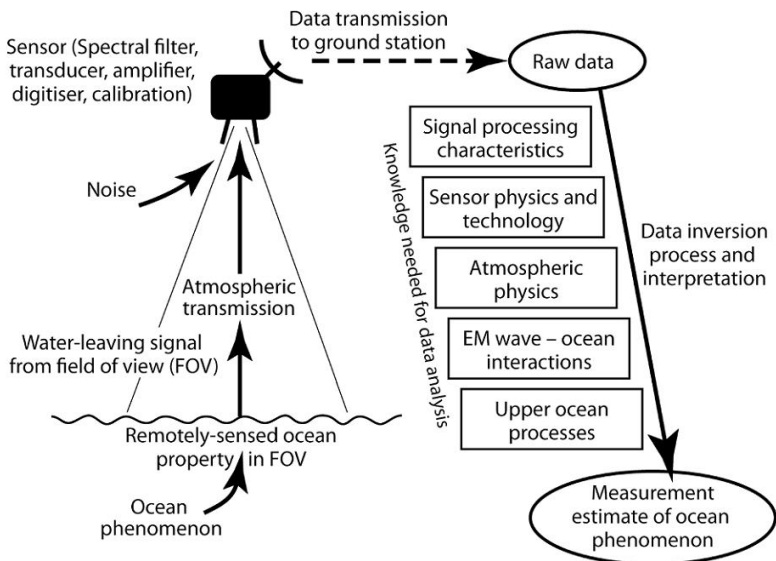


Figure 1. Scheme of information flow in ocean remote sensing. After Robinson (2010).

In order to convert the numbers received at the ground station into scientific measurements of useful precision and quantifiable accuracy, the remote-sensing process represented in the left-hand side of Fig. 2 must be inverted digitally using the knowledge and information identified on the right-hand side. It is their acquisition from a unique vantage point in space which gives satellite data their special character.

### *Capabilities of sensors on satellites*

Numerous possibilities have been open for scientists and users with the placement of ocean-viewing sensors on satellites. Main advantages that distinguish the satellite measurements from other earth observing techniques are: repetitive observations over the same area, wide coverage and relatively fine spatial resolution. Satellite missions in action provide data series that cover several years of observations presenting unique and otherwise unobtainable geoinformation. However, there are limitations that affect the scope of data possible to obtain through the remote sensing. To name some: the detector sensitivity, which pre-sets the sampling spatial characteristics; the other is the telecommunication systems specification that carry the data flow from the satellite to the receiving stations; the technical constraints of sensors and carriers constructions, their orbits and physical laws.

### *Creating image-like data elds from point samples*

The main objective of the space missions is to create two-dimensional images of the measured characteristic surface distribution which is easily interpreted by an end user and carries practical information in every segment of the image. Thus the image is constructed of point measurements of a variable of interest over a short time period. This requires the data to be received from one single sensor that guarantees the equal quality and precision of data throughout the image or a set of images. Otherwise, when more than one instrument is involved in the image composition the sensors have to be finely intercalibrated.

At a given moment of time almost all the sensors are making and instantaneous measurements of elements in the field of view (IFOV Instantaneous Field Of View) of a sensor. The IFOV is an area on the ground or sea surface relative to the pointing direction that is being captured by a sensor. This capture is a single measurement representing an average value over the IFOV area. By turning the sensor in reference to the platform or the ground in a set pattern the data

and coordinates are recorded to form a two-dimensional image. Due to these facts, the actual measured area is somewhat larger than the IFOV and depends on the time takes for a sensor to do a measurement and the speed of sensor movement (see Fig. 1). This “footprint” determines the spatial resolution of the sensor.

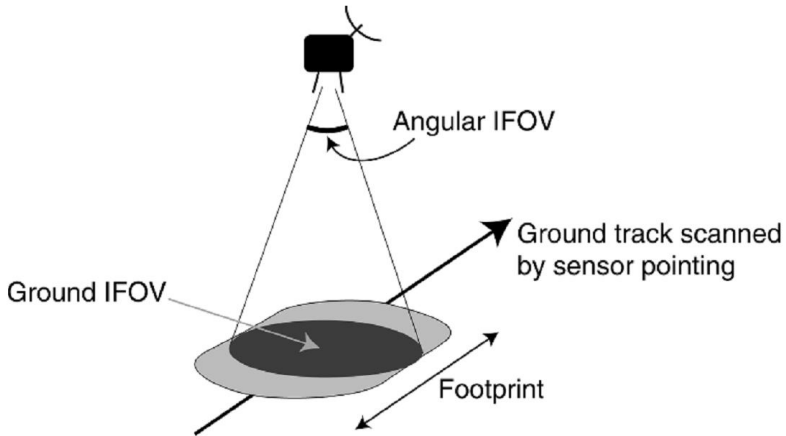


Figure 2. Sketch showing how the instantaneous field of view (IFOV) defines the measurement footprint during the sample integration time. After Robinson (2010).

There are sensors that only move in one direction over the ground and make measurements at equal time intervals in nadir direction. Nadir direction is coinciding with the direction of the force of gravity at a given point. An example of such a sensor is a nadir-viewing altimeter. This sensor produces only one point measurement over the time of measurement and thus doesn't produce an image-like footprint. The satellites carrying altimeters have a dense distribution of ground tracks that are being scanned in succession. The data are mapped to produce two-dimensional representations by collecting the sampling data over some period long enough to allow for sufficient density.

There are other types of sensors that provide truly near-instantaneous images of a variable distribution. These sensors scan the ground sideways across the satellite ground track. Normally the sensor rotation is adjusted in a way that the perpendicular scanning line width equals to the distance the satellite travels through the line-scanning time (see Fig. 3). This way the consequent cross-track lines form a continuous stripe of measurements. Every sideways scanning is represented by a succession of measurements made by rotating a sensor with a speed matching the speed of measuring. Thus the cross-track consistency

is ensured. The speed of measurement and the satellite ground-track speed are the parameters that preset the spatial resolution of a sensor. Due to technical difference each sensor has different spatial resolution and rotation speed. It is worthy of note that the footprint shape differs slightly with the scanning angle which makes the final geometry of an image not rectangular.

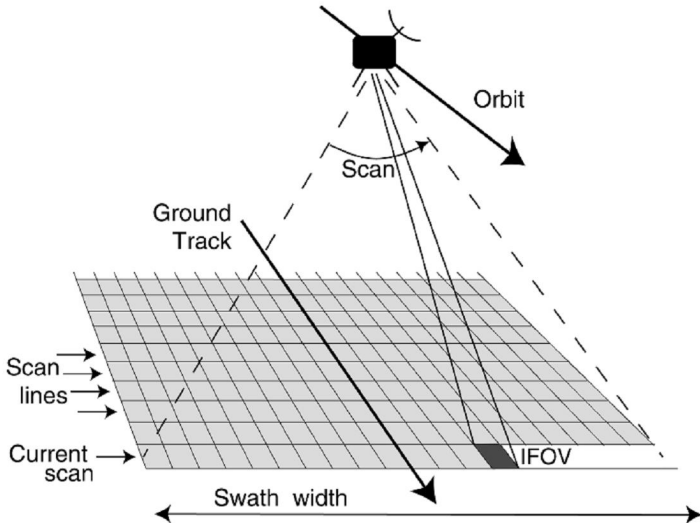


Figure 3. Swath-swing geometry of a rectangular, line-scanning sensor.  
After Robinson (2010).

As it is shown in the Fig. 3 the remote sensor obtains the information from an IFOV that possesses geometrical properties and represents an area of ocean or ground surface. Therefore the resulting values are space-time averaged values similar to the ones obtained by ocean simulating models, that represent a value as an average within a grid cell. This feature makes satellite measured values advantageous in regard to modeling needs in comparison to in-situ observations. However, satellite measurement validation procedure encounters the same problem as simulated results validation because of the large size of IFOV or grid cell and great spatial variability of natural environment parameters.

### *Satellite orbits*

Physical laws are friends and foes of space remote sensing. Gravitation and inertia are the forces that in simplified form can be expressed as

$$T = 2\pi\sqrt{\frac{r^3}{GM}}, \quad (1)$$

Here, the period,  $T$ , for a satellite to travel once round a circular orbit at distance  $r$  above the center of the Earth;  $G$  is the constant of gravitation;  $M$  is the mass of the Earth; and  $GM = 3.98603 \times 10^{14} \text{ m}^3 \text{ s}^{-2}$ . In terms of the satellite height  $h$  above the ground and the Earth radius  $R$  (about 6,378 km)  $r = R + h$  and so:

$$T = 2\pi\sqrt{\frac{(R + h)^3}{GM}}. \quad (2)$$

Ocean remote sensing satellites are being launched on two types of orbits: geostationary and polar. As it is clear from the name, geostationary orbit allows a satellite to hover over the fixed point on the surface of the planet. This is achieved by placing the platform at a height of about 35,785 km with a rotational period of approximately 23,93 hours (sidereal day). This is the time it takes the Earth to rotate around its axis. In a fixed position the sensor is able to effectively scan the area about 14 000 km in diameter with the center in a nadir point.

Per contra a near-polar orbit is placed much closer to the Earth surface (at about 700 - 1 350 km). The globe rotates almost across the satellite tracks which take about 100 min (Eq.2). Thus the satellite rounds the planet several times a day times a day with the tracks distributed evenly in a way to be re-sampled every next cycle (see Fig. 5). This way the measurements are building up in to timeseries, but this kind of a satellite never observes the ground between the tracks.

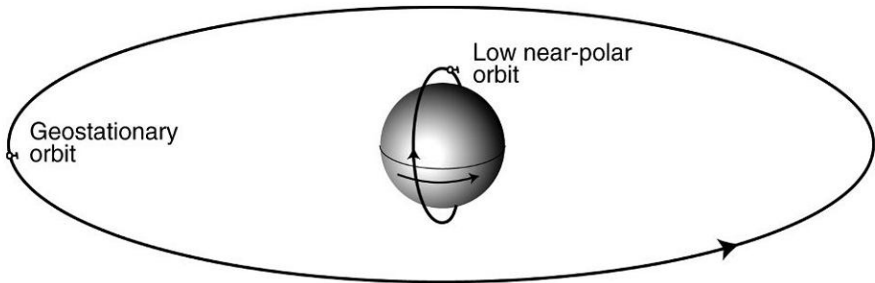


Figure 4. The two types of orbit used for Earth-observing satellites, drawn approximately to scale. The geostationary orbit is about 36,000 km above the Earth. The near-polar orbit is typically between 700 km and 1,000 km above the Earth surface. After Robinson (2010).

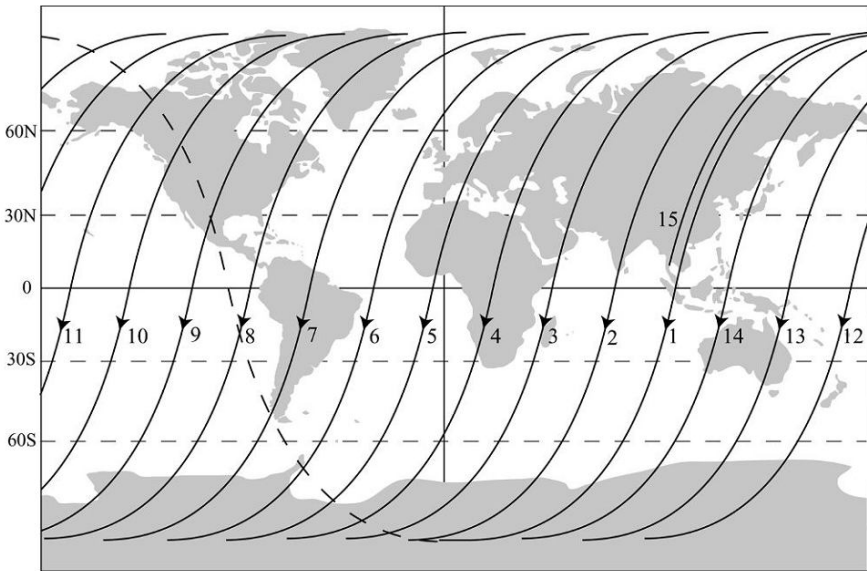


Figure 1.5. Ground track of a typical near-polar, low-Earth orbit, showing all the descending passes for one day and one ascending pass (dashed). After Robinson (2010).

For most applications it is convenient to design an orbit for a satellite to have a cycle of 3 to 35 days before the ground tracks coincide. These cycles are called repeat periods and the longer the repeat period the less the distance between ground tracks over the Earth surface and thus the larger the coverage. Thus there are missions with repeat periods of about 9,9 days (Jason), 35 days (Envisat), 105 days (Cryosat). In addition, mission orbits are often Sun-synchronous. This means that the image obtained from some ground or sea area is always taken at the same local solar time. It offers an advantage of similar insolation for images taken from the same spot, which simplifies the process of image processing. Though there is obviously seasonal variation of insolation through the year. However, due to the solar tide sun-synchronous orbit is discommended for altimetry missions, because the solar tidal phase will be exactly the same every time the satellite revisits the same location on the sea surface.

### *The space-time sampling capabilities of satellite sensors*

Though there are advanced technologies employed for space missions to observe the Earth surface, physical limitations make it impossible to obtain high resolution and frequent sampling at the same time.

For geostationary platforms the horizon limits the field of view as was explained earlier, but also the high position over the Earth surface restricts the sensor to 3 – 5 km resolution, on the other hand the revisit time for geostationary sensors could be reduced to 30 minutes.

Per contra a polar platform sensor is able of producing images that cover the whole globe in a case where a sensor swath is wide enough to cover distance between successive ground tracks. There is a possibility to obtain an image of the same spot more than once a day for a sensor with a wider swath due to overlapping areas (see Fig. 6a). Nevertheless even for the shortest repeat period it is technically difficult to gain a revisit period shorter then several hours. For the sensors that provide high resolution measurements (See Fig. 6b) the swath is relatively narrow. For those sensors it requires much longer repeat periods to obtain the whole globe coverage, therefore the revisit period extends to several days and more. Normally there is a balance between the resolution and revisit periods. For example, for altimetry missions the revisit time is sensibly short but wide areas of the globe are not covered at all.

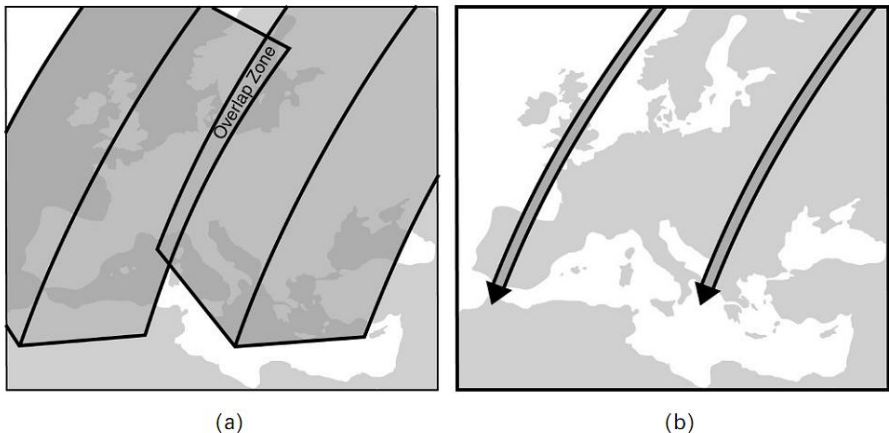


Figure 6. A single days coverage over Europe by (a) a wide ( $>2,000$  km) swath sensor and (b) a narrow ( $<200$  km) swath sensor. In each case the two tracks represent the typical spacing between successive orbits of a polar orbiter at an altitude of about 1,000 km.

After Robinson (2010).

For the types of sensors such as altimeters the longer the repeat period the better the spatial coverage therefore the data used for mapping the observational results allows for finer grid. However to build a map of a water body it takes much longer period and resulting composite maps are averaged over longer periods. While for the scanning sensors the resulting map resolution matches

that of a sensor resolution and depends on the sensor design and the orbit distance.

It is important to keep these limitations in mind when using the product built on the basis of satellite observations data or studying the raw data or building an ocean-observational system. Therefore when there is a need to obtain the data for the same ground area more frequent than two-three times a day the only way is to have two and more satellite on the orbit that can provide such sampling. This is obviously too expensive and therefore the reasonable space-time resolution should be aimed for. These constraints significantly limit the scales of the processes that can be detected and studied with the use of the satellite observations. For example, because of resampling time the processes with the life span shorter than the revisit period could be unregistered at all.

The summarized characteristics of time-space sampling can be represented as a rectangular area in a time-space chart as it is presented in the Fig. 7. Position and the size of the rectangle area are individual for each sensor and the platform it is carried on. The vertical axis represents a logarithmic lengthscale and the horizontal axis a logarithmic timescale. The lower boundary of the region allocated to a particular sensor represents the smallest spatial scale that can be detected by the sensor (i.e., its spatial resolution). Similarly the left-hand boundary represents the shortest time interval over which variations in the ocean can be detected (i.e., the temporal-sampling resolution). The bottom left-hand corner therefore represents the best spatiotemporal resolution that is possible using that sensor.

Represented chart is true under condition that there are no obstacles in the area of view of a sensor. The obstacles could be cloud cover for cloud sensitive sensors. Also the spatial resolution is assumed to be the one of the instantaneous capture of the surface characteristic, for example for along-track measurements the true area which the measurement is read from might be larger than the one represented. The right-hand boundary represents the timespan of the satellite operation, and depends on the lifetime over which useful data have been collected. In the examples illustrated a continuous series of at least 10 years is assumed. The region enclosed within the boundaries represents the space-time sampling space for that sensor. The height of the box indicates the range of lengthscales that can be studied with these data, and the width represents the range of timescales. Note that for the polar orbited satellites the lengthscale of the sensor is global. This kind of a diagram is used for considering the application which could benefit with the data of a particular sensor and for comparison of sensors.

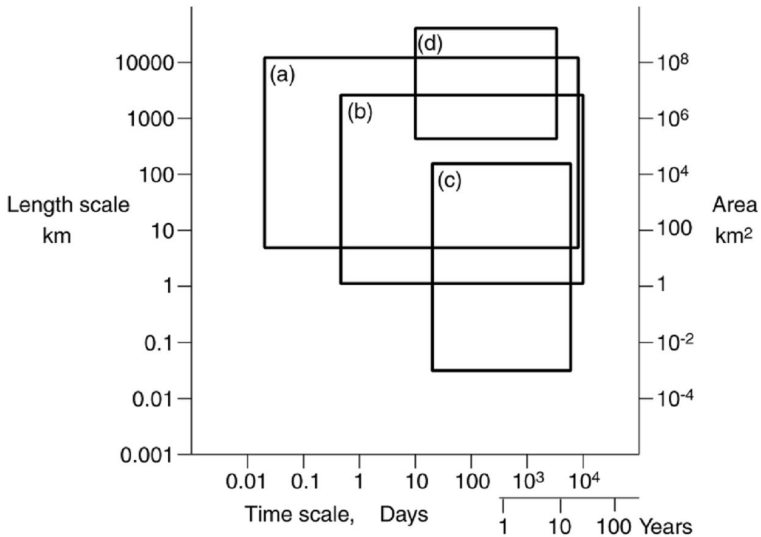


Figure 7. Diagram representing the space-time sampling characteristics of four types of sensor. (a) Scanning radiometer on a geostationary platform. (b) Wide-swath, medium-resolution (1 km) scanning sensor on a polar-orbiting platform. (c) Narrow-swath, near-resolution (20m) scanning sensor on a polar-orbiting platform. (d) Nadir-sampling non-scanning sensor (e.g., altimeter) on a polar-orbiting platform. After Robinson (2010).

## Remote sensing of marine environment

### *Main steps of satellite data processing*

There is a very narrow list of applications for raw remote sensing data usage. Most of end-users and researches deal with a range of processed products and data. The data processing includes calibrations, corrections, analyses, and resampling aiming to increase information efficiency and quality of data provided. Therefore a user has to be aware of the transformation the raw data is undergoing and the limitations and inaccuracies related to the processing. The aims of processing and levels of products are presented further on in the Fig. 6 and the Table 1.

### *Sensor calibration*

Calibration is the first stage of data processing that is intended to explicitly convert the electromagnetic property that a sensor is detecting in to a digital

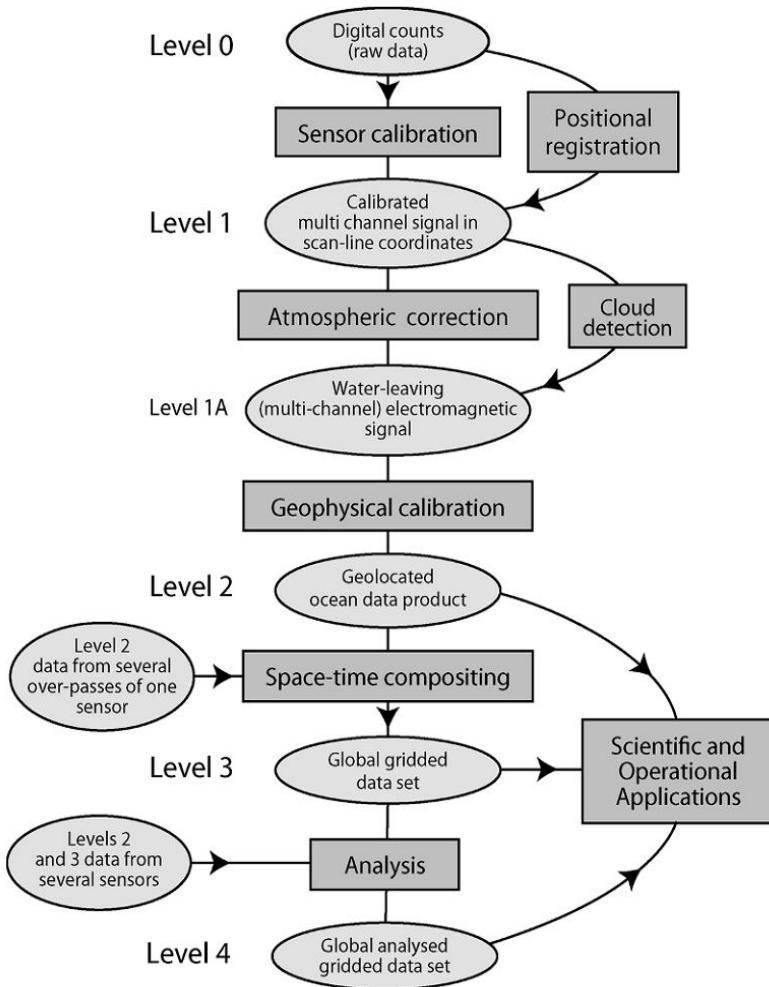


Figure 8. Outline of data-processing tasks to convert raw satellite data into ocean products. After Robinson (2010).

value which defines a physical property or parameter of environment. The calibration model is describing the interpretation of received radiation, phase or intensity into electromagnetic signal which is to be transmitted and received at the ground station. Though it is assumed that the transmission of a signal is faultless unless impossible, the conversion of a signal into a digital form is not hence the accuracy has to be estimated and presented along with the data.

**Table 1** Levels of satellite data products from deferent stages of processing.  
(after Lavrova et al.)

<i>Level</i>	<i>Description of product</i>
0	Raw data received from the satellite, in standard binary form.
1	Image data in sensor co-ordinates. Individual calibrated channels, of measurements made at the satellite.
1.5 (or 1a)	In special cases, level 1 data with atmospheric correction applied.
2	Atmospherically corrected and calibrated image dataset of water-leaving radiance or derived oceanic variable. Geolocated, but normally presented in image co-ordinates.
3	Composite images of derived ocean variable resampled onto standard map base. Averaged in space and time from several overpasses of level 2 data. Derived from a single sensor. May contain gaps.
4	Image representing an ocean variable averaged within each cell of a space-time grid, for which gaps at level 3 have been filled by data analysis including interpolation. The analysis may merge several level 2 and/or level 3 datasets from a number of sensors and may also use <i>in situ</i> observations or model output.

Before a mission launch every sensor on board the platform is being scrupulously calibrated. In-flight calibration is required for some sensors, because latter are subjected to degradation, displacement and so on. For example, radiometers are undergoing regular calibration against radiant sources to compensate the sensor degradation. Thus slow change in sensor sensitivity or representation is to be fully estimated a considerable time after the first set of data transmitted to the ground station. This obliges the raw data processing group to review and re-calibrate the data over and over again as the data builds up as well as the products which are derived from these raw datasets. Due to the nature of the data these products are not used by an end-user. These datasets are called level 1 products and made publicly available for remote-sensing technologies research.

### *Atmospheric correction*

The specific nature of the atmosphere is of a great concern for users of remote sensing from Earth observation satellites. The atmosphere is a medium which is not completely transparent for electromagnetic wavelengths and affects the

radiation being transmitted through it. There are, in fact, a few radiation wavelength windows through which the measurements are possible at all. Because of the complex composition of the atmosphere gases and impurities, such as dust, water vapor etc., each of which may absorb or scatter radiation affect the radiation characteristics or even absorb it completely. Thus the water vapor that forms the clouds prevents the ocean colour sensors from reading the surface, while for the other cases the estimation of the effect the atmosphere had on the radiation that had left the surface and reached the satellite becomes a complicated and crucial task.

### *Cloud detection*

The clouds mostly affect the infrared and visible spectrum measurements. To detect which pixel of the measurement is corrupted by a cloud and which is cloud free the cloud detection tests are run. Later are adapted for microwave measurements as well. Though clouds are transparent for microwave radiation; the cells of heavy precipitation are opaque for the later and need to be detected. Unfortunately pixels with cloud cover detected are beyond the restoration, and for such a pixel there is no way to retrieve the data with the use of satellite measurements only. To obtain the cloud-free dataset products there are several approaches used. First, it is possible to combine the measurements of two or more overpasses in a composite map, second is to apply some kind of analysis, such as optimal interpolation between cloud free pixels, and the third is the use of most recent cloud free overpass or other substitute for the data to fill in the cloud covered pixels. Often the combination of methods is used. These methods normally work well for a pixel that is completely covered by clouds or absolutely cloud free. In a situation when the pixel is only half covered it is often very hard to distinguish from clear sky conditions. Thus accepting the measurement from this pixel leads to erroneous dataset. Therefore for doubtful measurements it is safer to exclude those from the dataset. Yet it may seem quite a loss to abandon good data under suspicion of cloud contamination. Thus for operational use the suspicious data could be kept while for long term datasets, for example, climate studies, the cloud opaque data may corrupt the whole dataset. Methods to fill the cloud covered pixels are being chosen according to the application it is to be used for. A user has to be aware of the method used to prevent any erroneous conclusions drawn from a product. The clouds normally extend far beyond one pixel. Therefore it is important to check the “clear-sky” pixels as these are very likely to be affected by the atmosphere water vapor.

Also the atmosphere itself scatters light which results in backscattering of a signal that is emitted from the surface mostly in visible and near-infrared spectrum range. On the other hand the solar radiation that is progressing through the atmosphere towards the surface is being reflected back towards the orbit and registered by a satellite sensor as noise. These issues are of particular importance for infrared and microwave wavelengths, which are used to measure temperature. For each sensor the effect the atmosphere has on the registered signal differs which requires to apply different atmospheric corrections for each specific sensor. Unfortunately it is impossible to apply a 100% correction to a sensor as it is highly dependent on the content and the state of the atmosphere above the ground area that is sounded by a sensor. This is due to the fact that the state of the atmosphere isn't known with required accuracy. Thus the remote sensing measurements themselves are looked into as carrier of an atmospheric state and may reveal enough information to allow for sufficient correction. For that the use of multi-spectral channels becomes very important. By sampling in several different wavebands, chosen because of their different responses to both the ocean-leaving signal and the effect of the atmosphere, strategies have been developed which allow atmospheric variability to be accommodated under most conditions.

Being the basic correction the account for atmospheric influence produces datasets that are referred to as L1, L2 or L3 level products, however for recent missions water-leaving datasets with only the atmospheric correction applied are referred to as level 2 products.

### *Positional registration (Geolocation)*

Positional registration is the definition of geographical coordinates of the area measured, i.e. longitude and latitude of the field of view of a sensor. Often the positions registration is referred to as image navigation or geolocation. The process allows using the resulting measurement with a base map and because of that it is sometimes called geometric correction or rectification of the image. The accuracy with which this information is required depends on the application. According to the application the precision of positioning and the direction of the sensor pointing are calculated. For sensors that provide a single measurement for an area estimated as tens of kilometers in each direction the nadir position precision is required to be of several kilometers. For the other downcasting sensors which provide high resolution measurements the more precise nadir detection is needed. To obtain high precision geolocation ground stations are

tracking the satellites as well as satellite mounted sensors register the sensors pitch, roll and yaw. This information is sometimes collected, transmitted and even published with the satellite measurements.

The exact track of a satellite is called ephemeris. Due to modern improvements of geositional systems such as US system GPS (Global Positioning System) or Russian system GLONASS (Global Navigational System), it is possible to detect and calculate the position of a satellite. What is more complicated is to calculate the direction in which the sensor is pointing. Lack of such information makes the initial dataset, even with exact location of a sensor carrier, useless. Correction and calibration algorithms often use multispectral information in which the ratios or differences between different data channels is crucial. When resampling of an image onto a new geographical base is unavoidable it is important to resample each pixel, though the band ratio could be distorted. For these situations it is advisable to use “nearest neighbour” principle rather than averaged values from the surrounding pixels as this way the error wouldnt accumulate through the dataset.

### *Geophysical product derivation*

Only after the atmospheric correction and geolocation have been applied the actual ocean variable product stage begins. As the product a consumer is using for a specific application fundamentally differs from the measurement that a sensor makes the resulting variable should be considered as an estimate of a variable than a measure of electromagnetic radiation. This process is often called geophysical calibration and in practical terms it consist of applying of mathematical algorithms or rules to the calibrated and atmospherically corrected data registered by a sensor.

### *Development of calibration algorithms*

Geophysical calibration normally consists of combination of theoretical and empirical methods. As a basis for a calibration model it is often taken the theoretical basis of how the leaving radiation is influenced by an oceanographic parameter and how would it be transformed on its way to a sensor. For thermal measurements in the infrared range the theory of a black body emission of radiation provides the basis for satellite measurement interpretation. On the other hand the optical properties of the ocean and the atmosphere being well studied present such a complex model that it becomes almost impossible to offer a clear

calibration algorithm to assess suspended particles or sediment load. For active sensors the rough surface backscatter physical principle cannot be predicted or estimated by a known analytical function and so empirical approach is being called for. Of course it is desirable to design an algorithm with physically based clear theoretical model; nevertheless most of the estimations require in-situ measurements for calibration and generalization of measurements recorded by a sensor. Thus for an algorithm to be accepted for a range of application it has to provide results reliable enough to be used in different locations and under various conditions. Otherwise the principle and the algorithm would match location and condition of the calibration dataset origin and perform poorly for other locations and conditions. Once a geophysical calibration has been performed on satellite data from a single overpass, it is typically distributed as a level 2 dataset in its original native grid consisting of the original pixels arranged in rows and columns matching the sensor scan lines and the along-track direction of the satellite.

### *Ocean product validation*

Regardless the algorithm complexity and whether it is theoretically or empirically based it cannot be used for real applications unless it has been critically validated. Validation process defines the error statistics and therefore the bias and standard deviation of the data products derived from a satellite sensor. In the process the sensor readings are compared to a set of independent reliable set of measurements of the same property of the ocean.

In general the validation process represents comparison of in-situ measurements of a variable to a value of the same variable obtained with the use of a sensor reading. The readings should coincide in time and space with the ones obtained with remote sensing. The algorithm is to be tested for the whole range of values that it is designed for and thus it is required to perform the comparison for a large amount of measurements. This means that the good correspondence of the data in one region will not grant good validation for the global application. Hence the use of drifting buoys, or the use of long-transect ships of opportunity are advantageous for they provide information on measured variable in a variety of conditions and locations. This also applies to the atmospheric conditions and corrections, geolocation etc. Due to the sensor drift and to increase the data quality the validation process should be carried on through the whole lifespan of a sensor and must not include the data that the algorithm was developed on. Researchers and users of the final datasets have to ensure that the data product has been validated and provides the data quality suitable for an application.

### *Image resampling onto map projections*

For the data to be useful for a range of applications and be presented in a readable way the maps of ocean variables are constructed. Because this process doesn't affect the data quality or accuracy this stage is considered the least important of all. Geolocation stage of correction is called for to assign each pixel some geographical coordinates which makes the validation with in-situ observation possible and makes the information eligible for many applications. Most of the sensors provide the data that represent detailed view of the surface and is possible to print out on a screen or with a printer. However the image obtained directly is a rectangular representation of each pixel as they were captured by the sensor and organized in the rows and columns oriented the same way as the sensor was at the moment of measurement. In fact this rectangular image doesn't correspond to the actual ground area and after the geolocation may not appear to have distortions and be different in shape. This leads to a necessity to resample the image onto a convenient map projection and grid.

Map projection is normally being dictated by the user or an application the map is being published for. The problem of the taken image transfer from the spherical surface onto a flat surface is mainly due to the fact that every pixel is to be reshaped. Because of geometry change sometimes two pixels fit in to one mapping grid cell and the value has to be adapted respectively. On the other hand it happens that for some grid cell there is no pixel value at all. Therefore the process of transforming satellite data for mapping should be designed for no artifact information appears on the map and no information is lost.

It seems obvious that for the first case the weighted average should be used and the nearest neighbor interpolation for the latter case. However the ratio for different data channels (similar transformation for data obtained on different wavelengths) has to be preserved during transformation process to ensure correct placing of the values. For this situation it is advisable to use the "nearest neighbor" substitution which will preserve the original channel ration as was measured by the sensor.

### *Creating composite image maps*

To extend the use of satellite data beyond images or along-track measurements is to use the multiple data from the same sensor for several overpasses and from different locations. Using wider set of data allows compilation of images and measurements in a single composite map like a mosaic. Resulting map is referred

to as a level 3 product that is different from the level 2 products in several ways. The images are collected over certain period to cover a large region global or local, for example, seas. The resulting region exceeds the size of a swath or an image that is obtained during one pass above the region. The pixel size of such a product is normally larger than the native pixel in the level 2 image. The images used for the map are resampled in to a regular grid with northward orientation and common coordinates are assigned to pixels. Sometimes it contain statistical measures of the level 2 product variability such as standard deviation to describe the data from which the level 3 product has been composed. The resulting level 3 product often covers large areas and with the missing data (between the passes or due to data loss because of cloud cover etc.) filled with the data from other over passes.

Thus the thought should be given to the rules of how to deal with the multiple images for the same location. The algorithm which one follows for level 3 composition will affect the resulting product. First question to consider is how to deal with multiple entries of data from different images for the same pixel. Normally the values for one pixel are averaged and the longer the period of the integration the more level 2 values are averaged. However there are other ways of filling in the pixels, such as choosing the latest data or the data with the highest confidence level after application of all the corrections. The change of these rules may change the result significantly.

The next question in consideration is the time period for images integration and the pixel size. For some applications creation of different composite maps for ascending and descending overpasses is reasonable. Such situations are common for satellite with sun-synchronous orbits; here the maps may correspond to night and day passes. The choice made highly depends on the application the resulting map is intended. It has to be noted that the level 3 map doesn't contain all the information that is present in the level 2 product, nevertheless composite images are a useful tool for observing large events beyond synoptic scale that may not be represented by a limited geographical coverage of a level 2 product. The researchers and users of the level 3 product have to be aware of the rules applied to the composition of a level 3 product and consider implications they may impose.

Also it is reasonable to expect the composite map to have gaps resulting from inadequate coverage of the region or due to persistent cloud or other limiting effects. On the other hand it is more important to be sure that the data presented originates from the actual level 2 products and to be aware of the locations where it is not so. This is important for the composite images where the gaps

are filled with the interpolation method or the data is substituted by previous value or even climatological-averaged value.

Composite maps that use more than level 2 data find its applications and have to be referred to as level 4 product. The methods to fill in the gaps may include not only substitution and interpolation but numerical simulations and seasonal or yearly averages. Though the level 3 product should be composed on the data that the satellite sensor measured and no other sources and contain no gaps. The result allows estimation of the spatial distribution of a particular ocean variable during some fixed period of time and is called “analyzed field”. The data that is derived from the satellite measurements extend to the data from different types sensors and may even be blended with the in-situ observations. The smoothing and filling process apply a bias of expectations of what the fields should look like. However most of the users appreciate smooth and filled maps of an ocean variable there should be awareness of how those maps were obtained and what limitations and assumptions those apply. Averaging of a product leads to a loss of a high frequency variability while smoothing through a low frequency filter leads to a loss of low frequency signal and should be used appropriately. Most of the level 4 products have to provide the confidence level for each pixel to assist a user or researcher in drawing correct conclusions. This way the pixels that were filled with data other than derived from the sensor is expected to have lower confidence level.

### *Main sensors types used in remote sensing of marine environment*

Almost all the sensors mounted on ocean-viewing satellite platform are measuring electromagnetic radiation that leaves the sea surface. The wavelength which the sensor is sensitive to dictates the measured properties of the ocean; its resolution and sensitivity, the penetration through the atmosphere. The figure 8 presents existing sensors, their range of electromagnetic spectrum and windows of transparency for each of the sensors. The sensor groups, the electromagnetic part of the spectrum and the characteristics that are derived from these measurement are summarized in the figure 9.

Fig. 9 presents the atmosphere as a range of frequencies on which the transmittance of electromagnetic signal is possible and frequencies that are completely opaque for the signal and therefore the measurements are impossible. The “windows” where the transmittance is possible are not 100% transparent but allow for the signal to pass through. As one can see for the most of the wavelengths the signal cannot pass through the atmosphere. The “windows” exist at

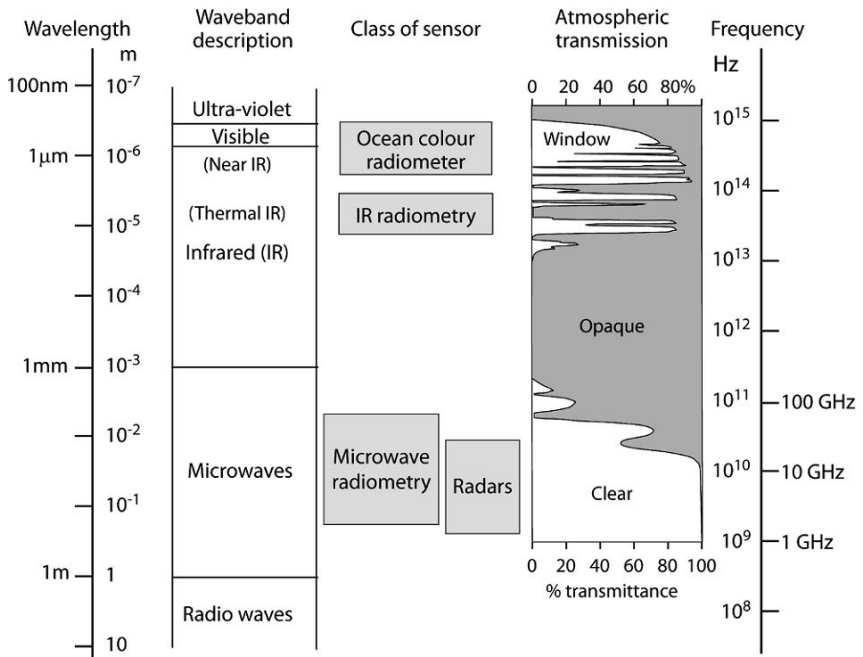


Figure 9. The electromagnetic spectrum, showing the regions exploited by typical remote sensing instruments. After Robinson (2010).

the wavelength of visible range from 400nm to 700 nm and near-infrared zone. These are useful to observe the sunlight reflected from the surface and the sensors for this zone of the spectrum belong to the ocean color sensors. Narrow windows between 3.5  $\mu\text{m}$  and 13  $\mu\text{m}$  are employed by IR radiometers and belong to the thermal part of the spectrum as the radiation at these wavelengths mostly depends on the temperature of the objects observed. In ocean remote sensing it is used for measuring sea surface temperature (SST).

For longer wavelengths the mankind has found applications such as TV and radio and mobile telecommunications; therefore this part of the spectrum is normally referred to as frequency than wavelength. These technological inventions exercise the fact that in these wavelengths the atmosphere is almost completely transparent. This part of the spectrum is called microwave region and for remote sensing some narrow bands of this spectrum zone have to be reserved according to international regulation. Microwave radiometers are passive sensors, monitoring the radiation emitted by the ocean, land and atmosphere. On the other hand radars are active microwave transmitters which emit

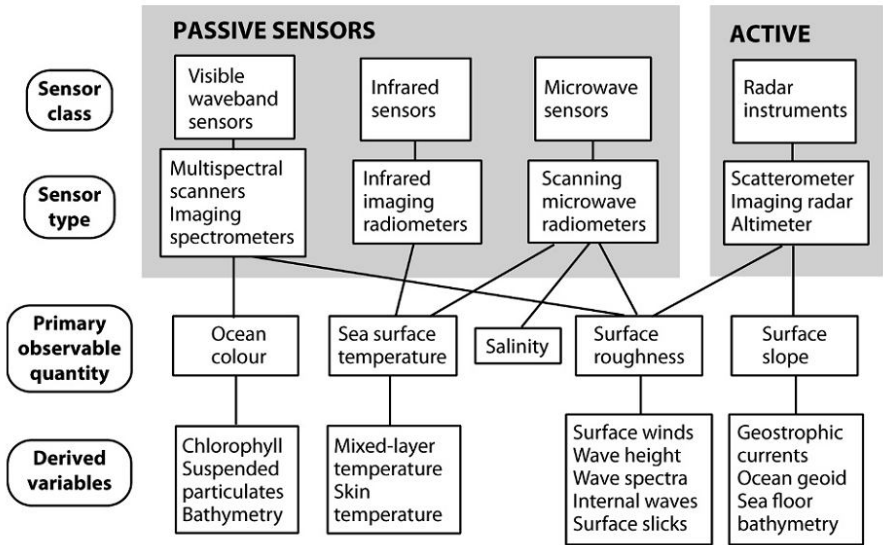


Figure 10. Schematic illustrating the different remote-sensing methods and classes of sensors used in satellite oceanography, along with their applications (from Robinson, 2004).

pulses and receive echoes from the surfaces they are facing. Receiver echo is then processed and to retrieve the information about the surface the signal has been reflected from. Some frequencies bare names in the form of letters as indicated in Table 2.

The radars differ according to the direction they point, length and modulations of pulses they emit and the analysis of the echo received by the radar. The main

**Table 2** Denition of common radar bands used for ocean remote sensing.

<i>Band</i>	<i>Frequency (GHz)</i>	<i>Wavelength</i>
L	0.390–1.55	19.35–76.9 cm
S	1.55–4.20	7.14–19.35 cm
C	4.20–5.75	5.22–7.14 cm
X	5.75–10.9	2.75–5.22 cm
K <sub>u</sub>	10.9–22.0	1.36–2.75 cm
K <sub>a</sub>	22.0–36.0	8.33–13.6 mm

two groups of radars differ due to the different direction of their view. The ones that point straight down underneath the satellite are called altimeters and their aim is to measure the height of the surface and the slope. The oblique pointing radars normally have angles of  $15^\circ - 60^\circ$  and scan the surface for the measure  $\sigma^\circ$  which represents the surface roughness. The roughness property is measured in relation to a specific frequency comparable with the wavelength it is measured with.

Sensors applications and capabilities are described in the following chapters. One can find the outline of the operational principles of the sensors while the most important information about data processing and interpretation is discussed more in detail. It is important to note that most of the sensors do not measure the ocean characteristic directly and those have to be derived through an algorithm. The derived variables are presents in the figure 10 bottom row.

## **Ocean colour**

### *Ocean color radiometers*

The basic principle of ocean color remote sensing is straightforward. The light measured by an ocean color sensor pointing towards the sea comes originally from the Sun. Some photons of light emitted by the Sun, with energies that place them in the visible part of the spectrum, enter the sea where they are either absorbed or scattered depending on what is contained in the seawater. Those of the scattered photons that emerge again give the sea its apparent color. This is quantied by a satellite ocean color sensor which measures the amounts of dierent wavelengths of light reaching it. A multispectral radiometer typically samples a limited number of narrow wavebands, chosen to capture the main structure of the spectral shape of incoming light (see Fig. 11). An imaging spectrometer samples in full detail across the spectrum, but such instruments have so far been used mainly onboard aircraft. From the relative magnitude of the water-leaving radiance detected by the dierent spectral channels of a radiometer, methods have been developed to estimate the concentration of those water constituents which give the sea its color.

The term ocean color is used loosely in remote sensing to refer to both the magnitude and the spectral composition of the light leaving the water. In practice it is the spectral radiance at the top of the atmosphere that is measured from a satellite. As shown in Fig. 12, this consists of light reected by the atmosphere, the sea surface, and (in very shallow water) the sea bed, as well as backscat-

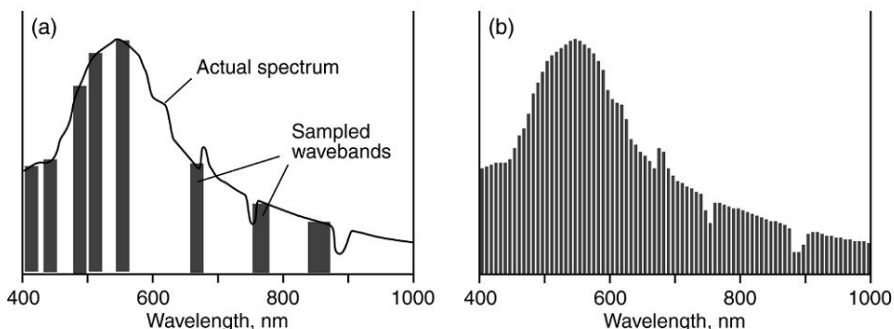


Figure 11. A typical spectrum of Earth-leaving radiance in the visible and near-infrared part of the spectrum, observed from a satellite above the atmosphere, as spectrally sampled by (a) a multispectral radiometer and (b) an imaging spectrometer with a spectral resolution of about 5 nm. After Robinson (2010).

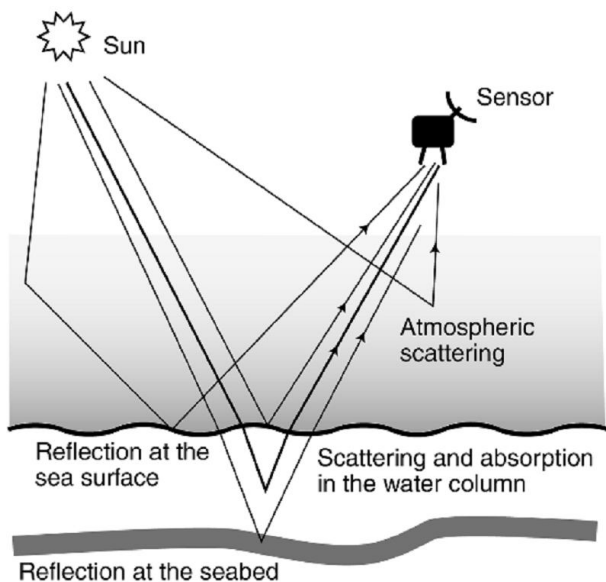


Figure 12. Factors which affect the light reaching an ocean color sensor. After Robinson (2010).

tered by seawater constituents. The retrieval of useful oceanographic quantities from top-of-atmosphere measurements is a challenging task, requiring careful separation of atmospheric scattering and surface reflection from true water-leaving radiance.

### *Atmospheric correction*

The greater part of the measurement of visible wavelengths of light made looking down from a satellite orbit comes from light scattered by the atmosphere into the field of view of the sensor, which may contribute more than 90% of total measured radiance. A proportion of the light leaving the sea surface is also scattered out of the field of view and so the atmospheric correction procedure must account for both these factors in order to estimate water-leaving radiance for each of the spectral bands recorded by the sensor.

That part of atmospheric correction due to scattering by air gas molecules themselves can be calculated directly for each pixel in the field of view of an imaging sensor, from knowledge of the relative positions of the Sun, the satellite, and the pixel. Scattering is also caused by larger particles of aerosols in the atmosphere. These may be water vapor or dust particles, but unlike atmospheric gases their concentration and distribution in the atmosphere is unknown and impossible to predict. Fortunately a technique has been developed which allows the variable contribution of scattering from aerosols to be estimated from measurements made by the sensor.

The key is to use radiance measured in two spectral bands from the near-infrared part of the spectrum. Because the sea readily absorbs almost all solar near-infrared radiation incident upon it, any light in these wavebands measured at the top of the atmosphere must have been scattered by the atmosphere or reflected at the surface. This can be used to estimate how much aerosol scattering has occurred in visible channels where the water-leaving radiance is not zero, and so the correction is accomplished. Thus near-infrared channels are essential for an ocean color sensor, although care must be taken to select the correct wavebands that do not overlap gas absorption lines in the spectrum.

### *Reflection from surfaces*

Part of the measured signal is reflected directly from the sea surface and this has no value for quantifying the water content. If the satellite detects direct specular reflection from the Sun it will dominate all other parts of the signal. Sun glitter prevents further analysis of the signal and must be avoided if at all possible, by careful selection of the orbit and sensor geometry in relation to the position of the Sun, and by tilting the sensor away from the Sun, bearing in mind that the extent of the Sun glitter region on the sea surface varies with the roughness of the sea.

Reflection from the sea surface of sky light (i.e., sunlight already scattered by the atmosphere) cannot be avoided. Instead corrections can be made for it within atmospheric correction. This means that knowledge of sea state (based on wind speed) is also needed for atmospheric correction. The other surface which may contribute reflections to the measured signal is the sea bed. Since sunlight is fairly rapidly attenuated with depth in seawater, by both absorption and scattering in the water column, reflection from the sea bed is only a problem when the sea is both shallow and clear. In most circumstances it is not an issue, but it can create problems when interpreting ocean color data in tropical, shallow seas. Where the water is very clear then bottom reflections in shallow seas can allow the color signal to be used to detect either the depth of the sea, the character of the sea bed (sand, coral, vegetation, etc.), or both but this is not a major application for global ocean color sensors.

### *Interpreting ocean color*

The color of the sea is not of itself an ocean variable of particular interest for most marine scientists. However, the factors which influence ocean color, such as the presence of phytoplankton, the concentration of pigments associated with primary production or dissolved organic material, and the concentration of suspended particulates are all of considerable oceanographic importance. Measurements of these properties can be derived from the color.

When atmospheric correction has been successfully applied to satellite ocean color data, the result is an estimate of the water-leaving radiance in each spectral channel in the visible waveband, normalized to reduce dependence on the Sun's elevation and the viewing incidence angle. Effectively, normalized water-leaving radiance should represent what a sensor would measure if looking straight down from an orbit that carries it just above the sea surface at the bottom of the atmosphere. This is what our eyes would detect as the color and brightness of the sea, ignoring any light reflected from the surface. The primary challenge of ocean color remote sensing is to derive quantitative estimates of the type and concentration of those materials in the water that affect its apparent color. Photons from the Sun, with EM energy corresponding to visible wavelength, enter the sea and eventually interact with molecules of seawater or its contents. The outcome will be either that the photon is scattered, in which case it may change its direction with a chance of leaving the sea and contributing to what the sensor measures, or it will be absorbed. The probability of scattering or absorption depends on the wavelength of the light and the material which it

encounters. The molecules within seawater tend to preferentially scatter shorter wavelengths of light (the blue part of the spectrum) and preferentially absorb longer wavelengths (the red end). This is why pure seawater with little other content appears blue. The pigment chlorophyll-a which is found in phytoplankton has a strong and fairly broad absorption peak centered at 440 nm in the blue, but not in the green.

Therefore, as chlorophyll concentration increases, more blue light is absorbed while green light continues to be scattered, and so from above the seawater looks greener. This is the basis for many of the quantitative estimates of seawater content derived from satellite ocean color data. The typical form of an algorithm to estimate the concentration of chlorophyll ( $C$ ) or phytoplankton biomass is:

$$C = A(R_{550}/R_{490})^B, \quad (3)$$

where  $A$  and  $B$  are empirically derived coefficients; and  $R_\lambda$  is reflectance (radiance coming out of the sea towards the sensor, normalized by incoming irradiance) over a spectral waveband of the sensor centered at wavelength  $\lambda$ . This is described as the green/blue ratio. In the open sea it is possible to estimate  $C$  to an accuracy of about 30% by this means. Most algorithms presently in use are somewhat more complex than (3) but are still closely related to it. If the sample data from which the coefficients and , etc. are derived is representative of many different open-sea situations then such algorithms can be applied widely in many locations.

Other substances which interact with the light and so change the apparent color of the sea are suspended particulate material (SPM) that has a fairly neutral effect on color except in the case of highly colored suspended sediments, and colored dissolved organic matter (CDOM, sometimes called yellow substance) which absorbs strongly towards the blue end of the spectrum. Both of these affect the light along with the chlorophyll greening effect when there is a phytoplankton population.

However, because the chlorophyll, CDOM, and SPM all co-vary within a phytoplankton population the green–blue ratio effect dominates the color and each of these materials can be quantified by an algorithm such as (3), as long as phytoplankton are the only major factor other than the seawater itself that affects the color. Such conditions are described as being Case 1 waters, and it is here that ocean color algorithms work fairly well to retrieve estimates of  $C$  from satellite data.

However, if there is SPM or CDOM present from a source other than the local phytoplankton population (e.g., from river runoff or resuspended bottom sediments), then we can no longer expect any simple relationship between the concentrations of these and  $C$ . In this situation green–blue ratio algorithms do not perform very well, if at all, and it becomes much harder to retrieve useful quantities from ocean color data using universal algorithms. These are described as Case 2 conditions. Unfortunately it is not easy to distinguish between Case 1 and Case 2 waters from satellite data alone. This can result in very degraded accuracy with errors of 100% if standard chlorophyll algorithms are applied in Case 2 waters. It is prudent to classify all shallow-sea areas as Case 2, particularly where there are riverine and coastal discharges or strong tidal currents stirring up bottom sediments, unless in situ observations confirm that Case 1 conditions apply.

An example of standard products derived from particular ocean color sensor representing main water quality parameters for the Ladoga Lake and the Neva Bay in the Eastern Gulf of Finland are shown on Fig. 13. These data were acquired on 8 July 2011 with Medium Resolution Imaging Spectroradiometer (MERIS) onboard ENVISAT satellite launched by European Space Agency (ESA).

The initial satellite data of 1 km spatial resolution (MERIS Reduced Resolution images) were processed with ODESA (Optical Data processor of the European Space Agency) software and visualized in BEAM software. As seen from Fig. 13, the southern part of the Ladoga Lake as well as the Eastern Neva Bay have increased amounts of all water quality parameters – chlorophyll  $a$  concentration (Fig. 3.3, b), yellow organic matter (Fig. 13, c) and total suspended materials (Fig. 13, d).

Another useful measurement that can be derived from ocean color is the optical diuse attenuation coefficient,  $K$ , usually denoted at a particular wavelength such as 490 nm (i.e.,  $K_{490}$ ). This is also inversely correlated with the blue-green ratio because the less the attenuation coefficient, the deeper the light penetrates before it is scattered back out, the more of the longer wavelengths are absorbed, and the bluer the water appears. The algorithms for  $K$  are similar in form to (3) and are somewhat less sensitive to whether the conditions are Case 1 or Case 2.

### **Sea surface temperature measurements from thermal IR radiometry**

Radiometers operating in the thermal infrared (IR) part of the electromagnetic spectrum observe the radiation which is thermally emitted by the sea surface, and so they are

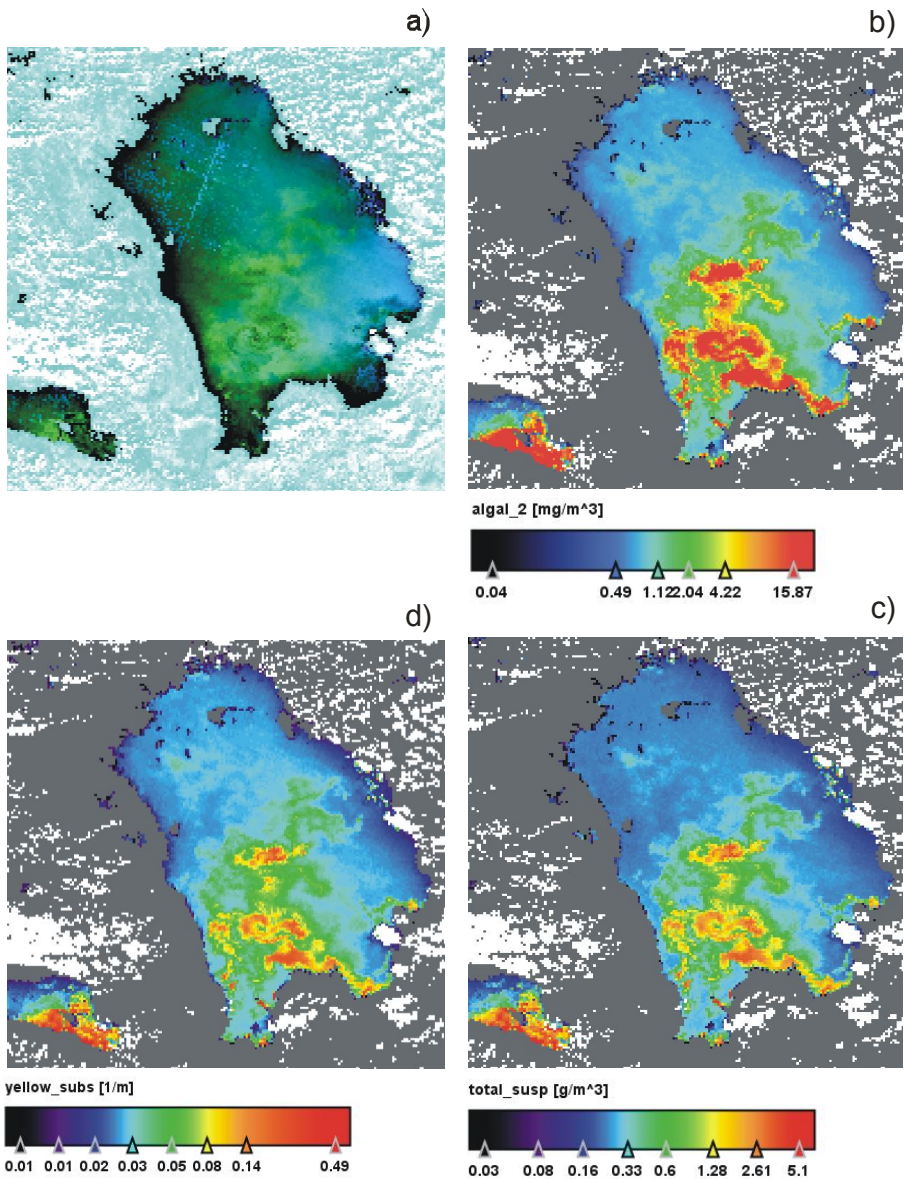


Figure 13. An example of standard ocean colour products derived from Envisat MERIS measurements taken over the Ladoga Lake and the Neva Bay on 8 July 2011 (08:59 UTC). a) colour composite image, b) spatial map of chlorophyll *a* concentration, c) spatial map of yellow organic matter distribution and d) spatial map of total suspended matter. © ESA

used to measure the radiation temperature of sea surface. The radiation measured by the IR radiometer can then be used to estimate the physical temperature of the water, because for IR measurements there is a close relationship between emitted infrared radiation and the sea surface temperature (SST) [Robinson, 2010]. Historically IR radiometers were primarily utilized by meteorologists to measure the temperature of clouds. After some time they proved to be useful for observing the spatial variability of SST patterns associated with fronts and eddies in the ocean under cloud-free conditions. Today IR SST measurements are routinely used to measure the true temperature of the ocean surface.

The major questions when deriving useful SST estimates from IR sensors is how to remove errors introduced by the atmosphere from sensor-measured infrared radiance and keep the SST records at high accuracy within a few tenths of a Kelvin. Another important issue is how to relate the temperature measured from space with the *in situ* surface temperature records with contact thermometers.

### *Basic physical principles of IR radiometry*

Naturally all surfaces, including the ocean surface, emit some radiation. The amount of the radiation emitted depends on the surface temperature and increases with increase of the surface temperature.

An infrared sensor records the radiance detected at the top of the atmosphere (TOA) in specific predefined wavebands (or channels). The individual radiation measurement in each channel is expressed as an equivalent black-body brightness temperature,  $T_{bn}$  [Robinson, 2010]. Black-body brightness temperature is the temperature at which a black body (a surface with 100% emissivity) would emit the same amount of radiance as was measured by the radiometer. For the particular wavelength, black-body emission is dened by the Planck equation:

$$L(\lambda, T) = \frac{C_1}{\pi\lambda^5 [\exp(C_2/\lambda T) - 1]}, \quad (4)$$

where  $L$  is spectral radiance per unit bandwidth centered at  $\lambda$ , leaving the unit surface area of the black body, per unit solid angle ( $\text{Wm}^{-2}\text{m}^{-1}\text{sr}^{-1}$ );

$\lambda$  is the wavelength (m);

$T$  is the temperature (K) of the black body;

$$C_1 = 3.74 \times 10^{-16} \text{ W m}^2;$$
$$\text{and } C_2 = 1.44 \times 10^{-2} \text{ m K}.$$

Integration of (4) over all wavelengths over the measured waveband is needed to represent radiance measured by sensor at particular spectral channel. However, it must be noticed that equation (4) address the radiation emitted by the black body (perfect emitter), which is an ideal theoretical concept, but not the real sea surface.

The emitting properties of any real surface can be described by its spectral emissivity,  $\varepsilon(\lambda)$ , which is the ratio of radiation emitted from real surface at temperature T (radiant flux density leaving a surface ( $\text{Wm}^{-2}$ ) to the radiation emitted by a black body at the same temperature T. In the IR part of the spectrum emissivity  $\varepsilon$  of sea water is very close to one and normally has a value between 0.98 and 0.99. In general,  $\varepsilon$  also depends on the incidence angle (decreasing with increase of the incidence angle), polarisation state (closer to one for vertical polarisation and lower for horizontal polarisation), wavelength (max. at about 10-11  $\mu\text{m}$ ), wind speed (decreasing with wind speed increase), and the presence of organic and oil films (decreasing with increase of film thickness).

Fig. 14 shows a spectral shape of Eq. (4) in the IR part of the spectrum and its variation with temperature for the range of typical SST. In general, the solar emitted radiation has a peak in the visible part of the spectrum. However, for the typical ocean temperatures (see Fig. 14) the emitted energy has a peak between 9  $\mu\text{m}$  and 11  $\mu\text{m}$  which makes IR part of spectrum an optimal region for monitoring SST.

In general, the IR instruments measuring SST usually look at the sea through two spectral windows in ranges of 3.5-4.1  $\mu\text{m}$  and 10-12.5  $\mu\text{m}$ , which have low absorption by the atmosphere. In these atmospheric window regions (shown in gray in Fig. 14) the influence of atmosphere on the passing radiation is small. The range of 10-12.5  $\mu\text{m}$  is often parted to two separate wavebands, 10.3-11.3  $\mu\text{m}$  and 11.5-12.5  $\mu\text{m}$ , which are usually called as the “split window” channels. Currently, all the main IR sensors measuring SST use these three channels. Most of them additionally have visible light channels to detect clouds or to map snow and ice.

As the emissivity of sea surface is a little less than unity, there is also a small portion of signal associated with reflection of sun and sky radiation from the sea surface in the total radiation measured by sensor. Reflected sky radiance can

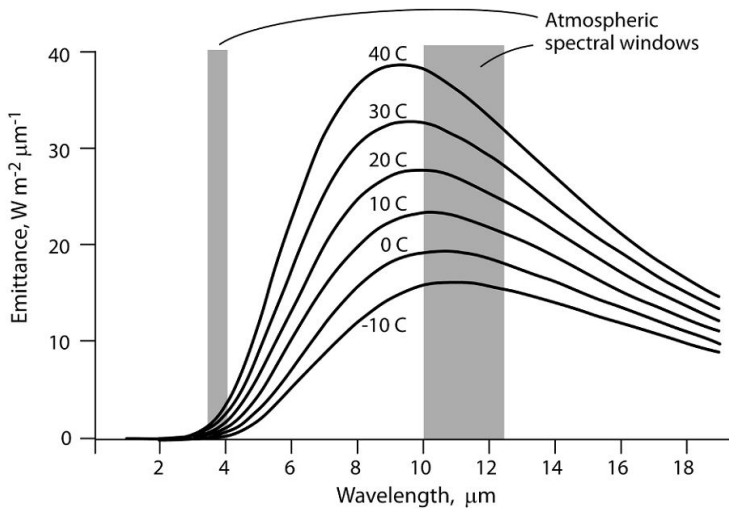


Figure 14. Black body emission spectra in the infrared part of e. m. spectrum at temperatures between  $-10^{\circ}\text{C}$  and  $40^{\circ}\text{C}$ . Gray bands - location of atmospheric windows. After Robinson (2010).

be easily removed while performing the atmospheric correction. The effect of reflected sunlight is different for different spectral windows. In the  $10\text{-}12.5\ \mu\text{m}$  infrared window the reflected sun signal is negligibly small, and this channel can be used both during the day and at night. For the  $3.5\text{-}4.1\ \mu\text{m}$  window, which has high sensitivity to changes in surface temperature and is much clearer than  $11\ \mu\text{m}$  window, reflected sunlight creates strong errors, and this channel is mostly restricted to nighttime observations.

#### *Attenuation of IR signal in the atmosphere*

While passing the atmosphere the initial radiation emitted by sea is influenced by the atmosphere. This happens even in relatively clear air. The primary sources of errors are clouds, water vapour, aerosols and other gases ( $\text{CO}_2$ ,  $\text{CH}_4$  and  $\text{NO}_2$ ). The last free atmospheric constituents partly absorb the radiation emitted by the sea and re-emit it at the colder temperatures. The absorption and re-emission of radiation strongly depends on the concentration of atmospheric constituents and local temperature of the atmosphere. In general, the absorption of the IR radiation by different atmospheric constituents has very strong space-time variation because the actual concentration of different atmospheric constituents strongly varies from day to day and from place to place. The main

effect of the atmosphere is therefore a reduction in the amount of the radiation reaching the sensor resulting in lower surface temperatures being recorded by spaceborne radiometer.

Dense clouds are totally opaque and completely block the radiation from the sea, and can be easily recognized. However, thin clouds and some small-size clouds could be a problem as they both lower the apparent sea temperature while being not very easily detectable. The challenging task then is to detect them and perform a correction of measurements. However, being invisible and thin, they could remain undetected in visible channels and lead to a relatively small reduction of the apparent sea temperature not distinguishable from some physical processes in the sea, e.g. upwelling or other low-temperature features. Undetected clouds lead to underestimation of the SST and may result in cool biases of order 0.5 K. Once clouds are identified with cloud detection procedure, the IR radiation for cloud-free pixels should be corrected for the influence of water vapor in the atmosphere to obtain accurate values of sea surface temperature. This procedure is called atmospheric correction. There are a number of techniques available for this; however, those mostly used are based on the fact that attenuation of IR radiation, e.g. by the water vapour, is different in different wavebands. For example, the radiation at 10.5  $\mu\text{m}$  is much more sensitive to water vapour than radiation at 3.7  $\mu\text{m}$ .

The condense in the cloud detection procedure is of the same importance as atmospheric correction for achieving accurate SST. Where there is some uncertainty remaining in cloud detection, corresponding pixels should be flagged and flagging information should be provided together with SST products. In general, cloud detection is more successful during daytime, when IR and visible light channels are used together, than at night.

### *Interpretation of satellite-measured SST*

Besides atmospheric effects, there is an additional problem for interpreting satellite-derived SST data related to the thermal structure in the top few meters of the ocean. Two prominent factors create near-surface vertical temperature gradients (Fig. 15). First, this is a diurnal thermocline which is developed on sunny calm days. Above diurnal thermocline is found a layer of about one meter thickness and having temperature about 1K warmer than water below. At night this warm layer disappears due to heat exchange with the atmosphere and gravitational mixing. Second effect, which is fully independent on diurnal thermocline, takes place at the top skin layer of the sea (upper 1 mm), where

the temperature is a few tenths of a Kelvin cooler than the water immediately below. This is called cool skin effect.

In general, there are different methods of measuring SST at different levels of the near-surface thermal structure (Fig. 15), each of them sampling a bit different SST depending on the measurement depth and time of the day.

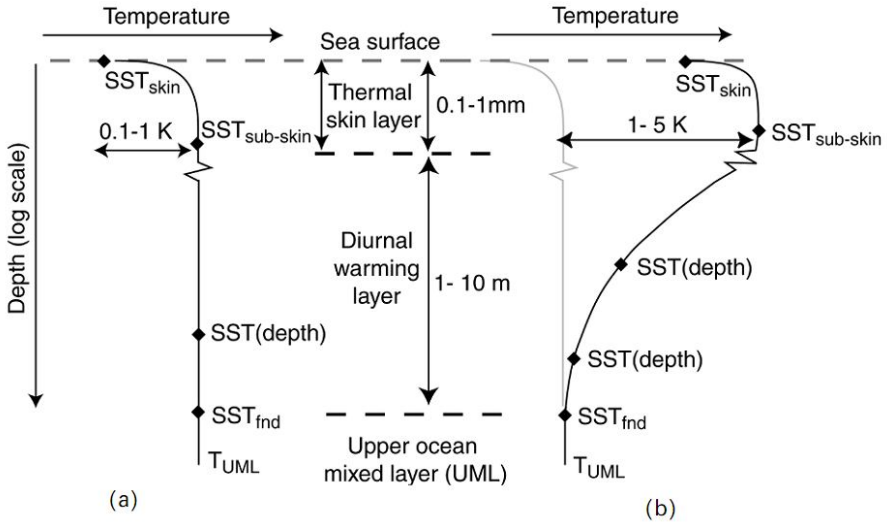


Figure 15. Characteristic temperature profiles at the sea surface for (a) nighttime conditions and (b) daytime calm light wind conditions and direct solar heating. After Robinson (2010).

In practice, it is valuable to distinguish between *skin SST*, the temperature in the top few microns, and *subskin SST* a short distance (of order 1mm) below the surface. These are separated by the thermal skin layer where heat transport is restricted to molecular conductivity because of the suppression of turbulence close to the surface. The subskin layer is typically a few tenths of a degree warmer than the skin layer. Infrared radiometers measure skin SST whereas microwave radiometers, receiving a radiation from deeper layer, approximately measure subskin SST.

### *Infrared SST data for marine environment research*

Nowadays the satellite IR SST measurements are the important data source for studying climate, basin scale, mesoscale and even finescale processes and phenomena in the coastal and open ocean environments.

In general 2-d fields of sea surface temperature measured by spaceborne IR sensors reveal any processes taking place in the ocean which affect the sea surface skin temperature under condition that the resulting effect on SST is large enough compared with the sensitivity of the detector, and the scale of process is longer than the spatial resolution of the sensor.

However, the presence of clouds strongly limits the utilization IR SST data specifically for monitoring mesoscale and coastal processes having relatively short time-scales. In such conditions any opportunity of cloud-free periods should be used to study the abovementioned processes. Though thermal IR SST data provides unique spatial details of SST distribution, the problem of clouds also limits the operational use of spaceborne SST measurements for the regions with persistent cloud cover, e.g. the Baltic Sea where the amount of cloud-free periods is only about 20-30 % throughout the year (Krežel et al., 2005; Kozlov et al., 2012a). Therefore it appears that the most effectively IR data could be used in combination with other types of remote sensing data, conventional in situ measurements and models filling the gaps resulting from the cloud cover. For the interpretation of IR SST data to get information about the ocean below the thermal skin layer one should understand the processes influencing surface temperatures. Main processes which potentially affect surface temperature and hence should be considered when analyzing IR SST data are schematically shown on Fig. 16.

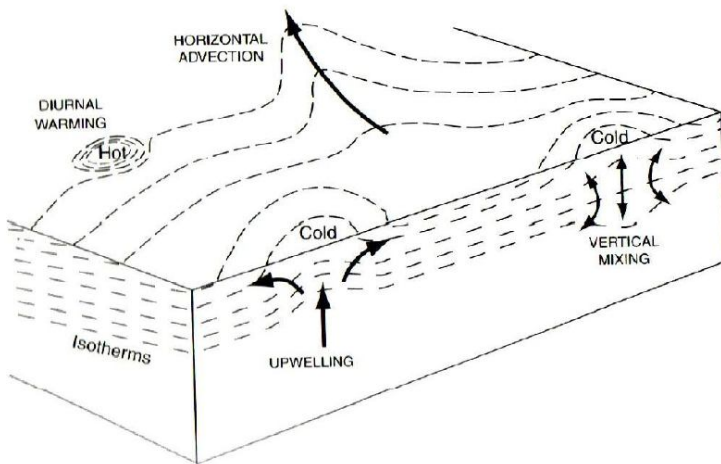


Figure 16. Local processes which can potentially influence the spatial distribution of SST. (After Robinson, 2004).

As seen from Fig. 16, spatial patterns observed in SST field may be produced by the horizontal advection of water masses having different temperature, e.g. when a large river discharges to the coastal ocean, or when a large ocean currents like Agulhas or Gulf Stream transport warm water over the large distances. Another important mechanism is the vertical advection affecting the surface temperature in e.g. upwelling regions. In such cases there will be a clear temperature signature of upwelled water which is always cooler the ambient water at the surface. An example of coastal upwelling evidenced in MODIS SST data with very pronounced SST signal in July 2006 for the SE Baltic Sea is shown on Fig. 17.

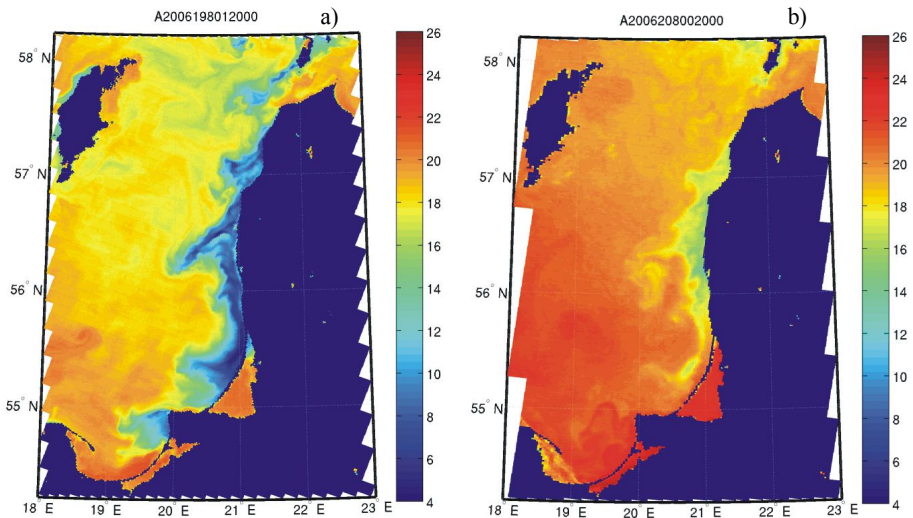


Figure 17. Coastal upwelling in the SE Baltic Sea as revealed by MODIS IR SST imagery in (a) its active development phase on 17 July 2006 01:20 UTC, and (b) relaxation phase on 27 July 2006. © NASA

The maps of MODIS SST on Fig. 17 depict the presence of a “narrow” area of cold waters adjacent to the coastline (Kozlov et al., 2012b). Strong SST drop about 12–14 °C between the ambient and upwelling waters in the coastal zone is clearly seen. On 17 July 2006 (Fig. 17, a) the upwelling front is perturbed by the development of several transverse filaments directed offshore, whereas during the upwelling relaxation on 27 July 2006 (Fig. 17, b) corresponding SST drop is much weaker but surface signatures of upwelling are still evident. Another process associated with the cool water reaching the sea surface from below and hence captured by satellite IR sensor is the vertical mixing. The

reason for its development could be a recent storm or breaking of internal waves in the open ocean both providing the energy for the mixing. In shallow shelf seas during the thermally stratified periods the energy sources for the vertical mixing are the tides and moderate wind events.

Finally, some SST patterns in satellite IR data can also be associated with the air-sea heat exchange through the sea surface. Among the most frequent events observed in SST data are the patches of warm temperature related to the intense sea surface heating during the calm sunny days and formation of diurnal thermocline.

### **Microwave radiometry**

As was noted before, radiation in the microwave (as well as in the thermal infrared) part of the e. m. spectrum is thermally emitted by the sea surface and can be used to measure the radiation temperature of surface. However, microwave radiometry has a more diverse range of oceanographic applications than infrared (IR) – it is able to measure not only sea surface temperature (SST) but also wind vectors, sea ice, rainfall over the sea, and even retrieve sea surface salinity (SSS). Moreover, all of this is achieved independently of cloud cover which is the main advantage of passive microwave radiometers (PMR).

The physical principles of PMR are very similar to those for the IR radiometers. Microwave radiometers operating at wavelengths between 1.5 mm and 300 mm (200 GHz – 1 GHz) register the thermal radiation in the microwave part of the spectrum naturally emitted by the sea surface. However, at the top of atmosphere (TOA) the microwave sensor also receives a portion of the microwave radiation emitted by the atmosphere, another portion which is reflected by the sea surface from atmospheric and solar emission, and also some signal related to the background radiation from cold space (Fig. 18).

At properly chosen wavelengths there is almost no atmospheric influence (absorption and scattering) on the microwave signal. However, presence of liquid water can strongly attenuate the signal at particular wavebands, which in turn can be used to detect the vertical profiles of temperature and moisture in the atmosphere. The ability of PMR to see through clouds is balanced by the coarser spatial resolution if compared with IR radiometers. This comes from the fact that thermal emission, and consequently the signal received by the sensor, is weaker in microwaves. To maintain the signal strength over the noise level, the field of view (FOV) for microwave radiometers should be considerably wider which leads to a poorer spatial resolution typically being 25-50 km.

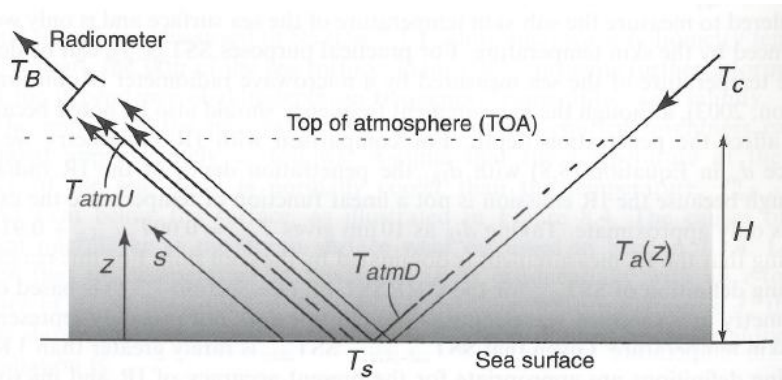


Figure 18. Contributions to the brightness temperature (TB) measured by microwave sensor at the top of atmosphere (TOA) from the sea surface ( $T_s$ ), cold space ( $T_c$ ) and atmosphere ( $T_{atmD} + T_{atmU}$ ).  $T_{atmU}$  is upward atmospheric radiation at the TOA and  $T_{atmD}$  is the downward atmospheric radiation incident on the sea surface. After Robinson (2004).

### *Physical principles of microwave radiometry*

Microwave radiation emitted from a surface is often referred to as *brightness temperature* (the temperature of the black-body that would emit the radiance measured by satellite sensor). In the microwave wavebands emissivity for the sea surface is  $\varepsilon < 0.5$  (unlike  $\varepsilon \approx 0.98$  in the thermal IR region). Emissivity depends on the viewing incidence angle relative to the local surface slope, the dielectric constant of seawater, and temperature. As the dielectric constant in turn depends on temperature, the dependence of microwave brightness temperature on subskin SST is not linear. Moreover radiation may change if the mean square surface slope or surface salinity changes, even if the SST remains constant. While this is a drawback for measuring SST, it opens the possibility of using microwave radiometers for detecting sea surface roughness and salinity. Fig. 19 summarizes different environmental factors influencing emission of microwave radiation from the sea surface and its passage through the atmosphere.

### *Elements of microwave radiometers*

Microwave radiometers are passive devices measuring the power of the continuous electromagnetic radiation incident upon their detectors. They sample within specific narrow-frequency bands, and some of them are able to measure

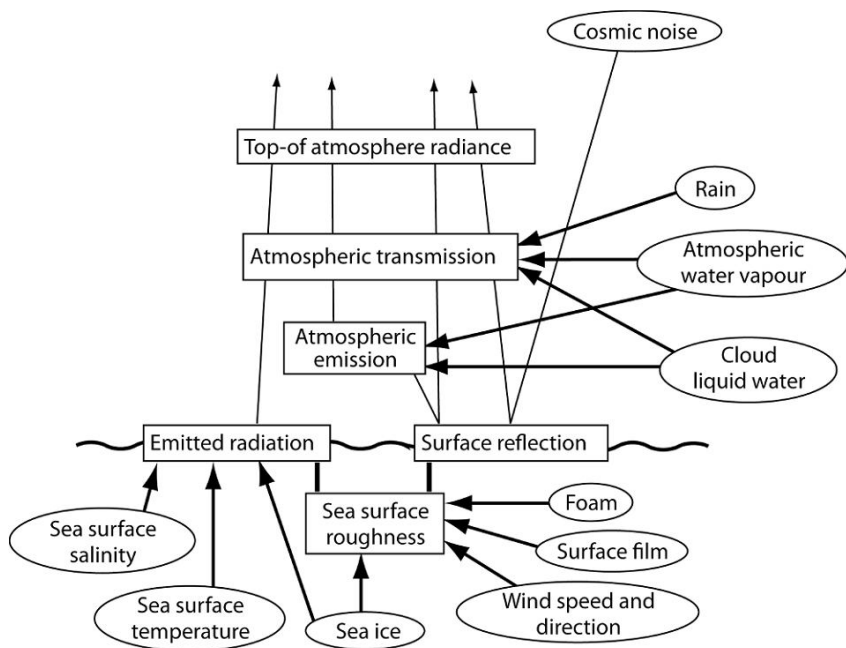


Figure 19. Schematic showing main environmental factors influencing the emission of microwave radiation from the sea surface and its passage through the atmosphere. After Robinson (2004).

separately the power in different polarizations. The spatial resolution for PMR is between one and two orders of magnitude poorer than for an IR radiometer. Because of poor focusing, microwave radiometers are not reliable within about 100 km of land.

### *Retrieving geophysical quantities from microwave radiometers*

From the PMR measurements of brightness temperature it is possible to infer different contributions of SST, surface roughness, and salinity, as well as to identify and assess atmospheric contamination by liquid water, because each of these factors differentially affects different microwave frequencies. For example, SST strongly affects wavebands between 6 GHz and 11 GHz, and the effects of salinity are found only at frequencies below about 3 GHz. Surface roughness influences frequencies at 10GHz and above, and also depend on polarization. Thus a multifrequency and multipolarization radiometer can, in general, be used to

measure SST, surface wind, and precipitation. The retrieval of useful oceanographic measurements is based mainly on using empirical algorithms, developed from matchups between in situ observations and satellite data [Robinson, 2004]. Mapping of sea ice is another important application of PMR. The key factor here is that the microwave emissivity, and hence the brightness temperature, of ice and snow is higher than that of the sea surface. Fig. 20 shows the sea ice concentration map over the Arctic calculated from AMSR-E radiometer data using the Artist sea ice algorithm (Sprenn et al., 2008).

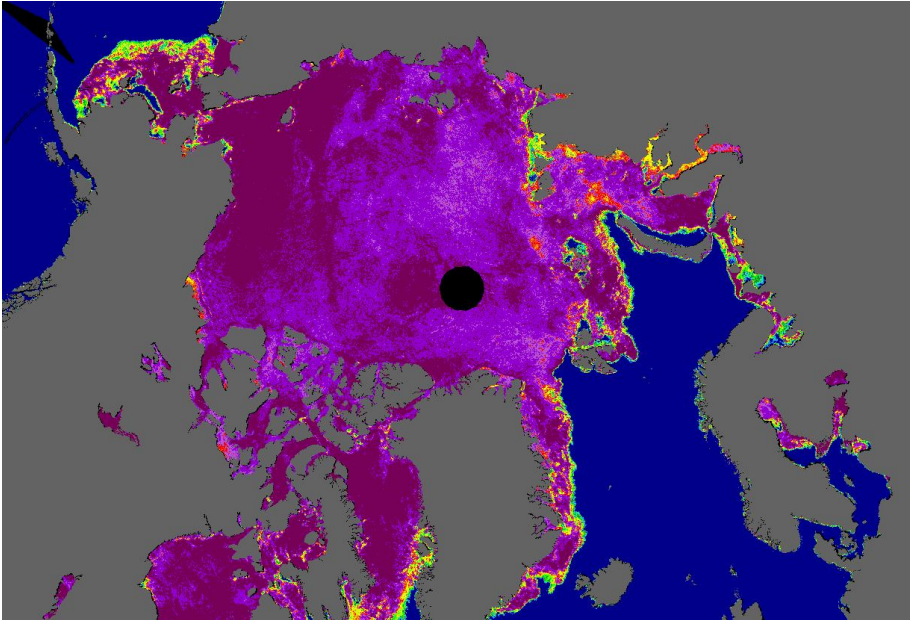


Figure 20. Sea ice concentration map over the Arctic from AMSR-E microwave radiometer data. © University of Bremen.

## **Radar basics. Altimetry. Scatterometry. Synthetic Aperture Radar**

### *Introduction to radars*

Radars are active microwave instruments which use the energy in the form of e. m. waves in the microwave part of the spectrum to create and emit pulses towards the sea surface and then to measure the reflected echo. They operate typically between P-band at about 300 MHz and K-band at about 30 GHz. The

microwave energy is directed towards the ground, either directly below the sensor, in the case of nadir radars, or obliquely.

The utility of radars depends on the character of the pulse that is emitted. It also depends on what properties of the reflected pulse are measured (Fig. 21). The timing of the returned pulse after reflection from the sea surface enables the distance between the radar and the point of reflection to be measured. For a nadir-pointing radar this enables to estimate the height of the sea surface. This type of radar is called altimeter. For oblique-viewing radars the returned signal is dispersed in time according to the distance to the point of reflection.

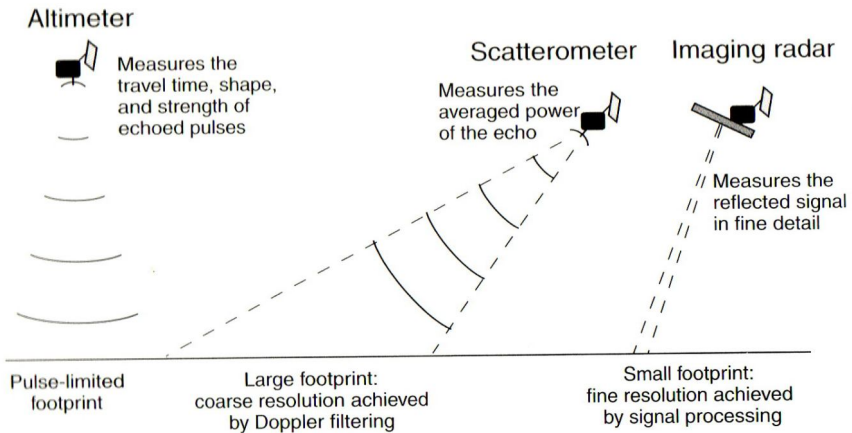


Figure 21. Different types of radars used for Earth observation. After Robinson (2004).

The magnitude and polarisation of the reflected pulse depends on the properties of the sea surface, and to the most it is a measure of the surface roughness. Oblique-viewing radars measuring the scattered back signal (also called radar backscatter) are classed in two categories. Those measuring average backscatter from a wide field of view are called scatterometers, and are used primarily to measure the wind speed and direction. Second class are radars with much finer resolution, called imaging radars, they provide maps of sea surface roughness capable of imaging a variety of small and mesoscale ocean phenomena.

For nadir-viewing radars, the shape of the returned pulse contains information about statistical distribution of surface elevation within the footprint, and hence enables altimeters to provide a measure of the ocean wave height.

In general, radars for measuring the ocean are often treated as completely weather-independent sensors for which atmospheric effects are negligible. It is true

that radars are not restricted by clouds as visible and IR radiometers, however some atmospheric effects still take place in some microwave sub-regions.

### *Interpreting radar backscatter measurements*

The magnitude of the radar echo reflected from the sea surface is expressed as a variable called the normalized radar backscatter cross-section, usually referred to by the symbol  $\sigma_0$ . After calibration, the data from a radar yield estimates of, either as single averages for a given field of view or as an array of many samples mapped over the sea surface. The size of depends on surface roughness and in particular on the amplitude of short waves on the sea surface propagating in the radar ground range direction and having a wavelength of  $\lambda$  — where  $n$  is 1, 2, etc.;  $\lambda$  is the radar wavelength; and  $\theta$  is the radar incidence angle. This is the Bragg resonance mechanism, as a consequence of which different radar frequencies produce different magnitudes of echoes from the same sea surface and same incidence angle.

Fig. 22 illustrates broadly how  $\sigma_0$  varies with incidence angle under different wind conditions or sea states. The behavior of  $\sigma_0$  can be separately characterized in three ranges of incidence angle. At low incidence angles (a) specular reflection appears to be the dominant process. For a very calm sea there is a very narrow angular response giving a very high return at  $0^\circ$  incidence which rapidly drops off as the incidence angle increases. For a somewhat rougher surface under moderate winds the nadir-viewing response is weaker, but does not decay so rapidly with increasing viewing angle, so that within a few degrees from normal incidence it is reflecting more power than the air at surface. The very high sea state continues the trend, with an even lower  $\sigma_0$  at  $0^\circ$  but very little drop-off with incidence angle. This is the way in which the magnitude of altimeter pulses responds to surface roughness. In a central region of the diagram (b) at incidence angles between about  $20^\circ$  and  $70^\circ$ , appropriate for most oblique-viewing radars, the behavior of  $\sigma_0$  is quite simply described. At a given  $\theta$  it increases with sea state, while there is an approximately linear reduction with increasing viewing angle, except for a calm sea that is already very low. Finally at incidence angles greater than  $70^\circ$  (c) the value of  $\sigma_0$  appears to drop off more rapidly with  $\theta$ , reaching very low values at grazing incidence approaching  $90^\circ$ . The broad dependence on sea state, albeit different in different bands of viewing angle, is what makes such a useful parameter for marine remote sensing.

Note that in practice  $\sigma_0$  depends also on other parameters such as frequency and polarization, so Fig. 22 is not intended to be precise.

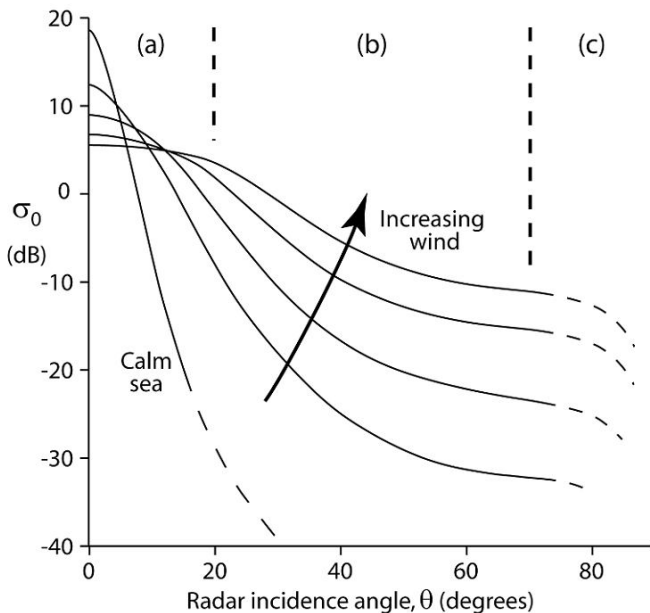


Figure 22. Sketch of typical measurements of  $\sigma_0$  as a function of incidence angle and sea state. The curves show the responses to different winds. After Robinson (2010).

## Altimetry

A satellite altimeter is a nadir-viewing radar which emits regular pulses and records the travel time, the magnitude, and the shape of each return signal after reflection from the Earth's surface. Travel time is the essential altimetric measurement, leading to determination of the ocean surface topography at lengthscales longer than about 100 km. Ocean surface topography contains information about ocean dynamical and geophysical phenomena. If the travel time can be measured to a precision of  $6 \times 10^{-11}$  s then, knowing the speed of light, the distance can be calculated to a resolution of 1 cm. Corrections have to be made to allow for the changed speed of light through the ionosphere and the atmosphere, and for delays associated with reflection from a rough sea surface (Chelton et al., 2001). It is generally agreed that for these corrections to approach the target accuracy of 1 cm a dual-frequency altimeter must be used (to determine ionospheric refraction), and a three-channel microwave radiometer is needed to sound water vapor in the atmosphere.

The altimeter is not an imaging sensor. Viewing only the nadir point below the satellite, it simply records measurements of distance between the satellite and the sea surface along the ground track. The spatial and temporal-sampling characteristics therefore depend entirely on the exact orbit repeat cycle of the satellite. This was chosen to be about 10 days for the TOPEX/Poseidon (T/P) and Jason altimeters which fly on platforms dedicated to the altimetric mission, although for other altimeters it has ranged between 3 days, 17 days, 35 days, and longer. The longer the revisit interval the finer the spatial-sampling grid. Typically, ocean topography data are interpolated onto a geographical grid and composited over the period of an exact repeat cycle, to produce images which are comparable with global SST or ocean chlorophyll composite images although produced in a completely different way.

By itself, knowing the distance  $R_{alt}$  between the ocean surface and a satellite is of limited value. Fig. 23 shows what else needs to be defined or measured for this to yield an oceanographically useful property. First of all, when the height of the satellite,  $H_{sat}$ , is known relative to a reference level, then the height,  $h$ , of the sea above the reference level can be determined. The reference level is a regular ellipsoid-shaped surface defined within a frame of reference fixed in the rotating Earth. It is chosen to match approximately the shape of the Earth at sea level, and provides a convenient datum from which to measure all other heights.

Several physical factors contribute to  $h$ , which is called the ocean surface topography. The first is the distribution of gravity over the Earth, as represented by the geoid, at height  $h_{geoid}$  above the reference ellipsoid in Fig. 23. The geoid

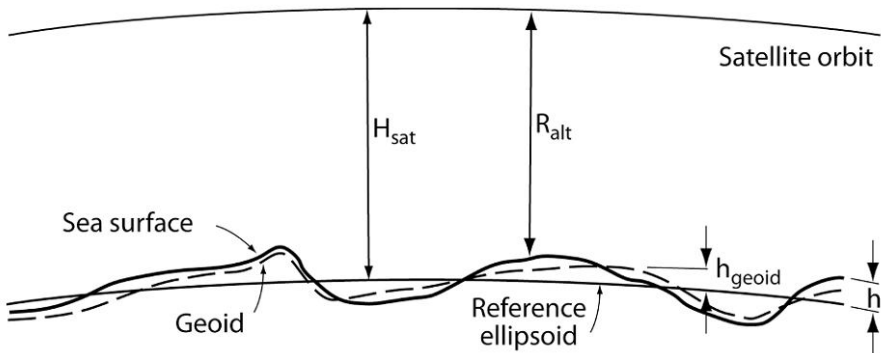


Figure 23. The relationship between different distance quantities used in altimetry. After Robinson (2010).

is the equipotential surface, at mean sea level, of the effective gravitational field of the Earth which incorporates Earth rotation forces and the gravitation of the solid Earth, the ocean itself, and the atmosphere. By definition it is normal to the local effective gravity force, and if the ocean were everywhere in stationary equilibrium relative to the Earth, its surface would define the geoid.

Another factor which contributes to  $h$  is  $h_{tide}$ , the instantaneous tidal displacement of the sea surface relative to its tidally averaged mean position, including the contribution of the Earth tide. A third is the local response,  $h_{atm}$ , of the ocean to the atmospheric pressure distribution over the ocean, approximated by the inverse barometer effect in which an increased pressure of 1 mbar lowers sea level by 1 cm. The remaining factor is displacement of the sea surface associated with the motion of the sea, called the ocean dynamic topography  $h_{dyn}$ . Thus:

$$h = h_{dyn} + h_{geoid} + h_{tide} + h_{atm}. \quad (5)$$

The dynamic topography is the property which is of most relevance for ocean modeling since it contains information about ocean circulation. Rearranging (5) and substituting  $h = H_{sat} - R_{alt}$  yields:

$$h_{dyn} = H_{sat} - R_{alt} - h_{geoid} - h_{tide} - h_{atm}. \quad (6)$$

The accuracy and precision of the estimated ocean dynamic height depends not only on the altimetric measurement itself but also on the other four terms in (6). For dedicated altimetry missions flying at a height of about 1,340 km where atmospheric drag is minimal, the height of the satellite in orbit,  $H_{sat}$ , can now be predicted to a precision of 2 cm using a combination of laser and microwave-tracking devices and an orbit model using precise gravity fields. The tidal contribution has been evaluated along the repeat orbit track by tidal analysis of the altimeter record spanning several years. Because tidal frequencies are very precisely known the response to each constituent can be evaluated to an accuracy better than 2 cm in the open ocean, even though the sampling interval of about 10 days is longer than most tidal periods. This is only possible when the precise period of the repeat cycle is chosen to avoid any serious aliasing with one of the major tidal constituents. For this reason a Sun-synchronous orbit, which aliases the S2 (solar semidiurnal) tidal signal, should not be used. Over shelf seas where tides are very high and can vary rapidly over short distances it is not so easy to remove the tides and so the estimate of dynamic

height is less accurate. Atmospheric pressure correction is based on the output of atmospheric circulation models.

### *Evaluating sea surface height anomaly*

Currently the geoid has been measured independently, but not yet to a very high precision, and so oceanographers must be content with measuring the combined  $h_{dyn} + h_{geoid}$ . Of these, the typical magnitude of the spatial variability of  $h_{geoid}$  is measured in tens of meters, about 10 times greater than that of  $h_{dyn}$ , which is why until recently the time-mean ocean topography from altimeters provided geophysicists with the best measure of the geoid. However,  $h_{geoid}$  does not vary with time, at least not sufficiently to be detected by an altimeter over tens of years, whereas the time-variable part is comparable in magnitude with the mean component, of order meters over a few months.

Therefore the time variable part of  $h_{dyn}$ , called the sea surface height anomaly, SSHA, can be separated from the measured  $h_{dyn} + h_{geoid}$  by simply subtracting from it the time-mean sea surface height over many orbit cycles ( $MSS = Mean\{h_{dyn} + h_{geoid}\}$ ). To enable a time-mean to be produced, the orbit track must be precisely repeated to within a kilometer and the data must be accumulated from several years of a 10-day cycle. For this reason it is essential to fly a new altimeter in precisely the same orbit as its predecessor so that the mean surface topography of the earlier mission can be used straight away. Then SSHA can be calculated from the first orbit cycle of the new altimeter, without having to wait another few years to build up a new mean topography for a different orbit track. It is important to remember that the SSHA, which is widely used for oceanographic analysis and is assimilated into dynamical ocean models, does not contain any information about the dynamic height of the ocean associated with the mean circulation. Global maps of SSHA do not display the dynamic topography signatures of the strong ocean currents at all, apart from the fact that the eddy-like activity is strongest where the major currents tend to meander. There are presently three families of altimeters in operation, as listed in Table 3, with details of their attitude, orbit repeat, and approximate accuracy (root mean square) of an averaged SSHA product. The T/P–Jason family is a joint French/U.S.-dedicated altimetry mission in a high non–Sun-synchronous orbit. In contrast the Geosat and ERS series are on lower Sun-synchronous platforms for which orbit prediction accuracy would be, on their own, much poorer. However, because these satellites cross over each others orbit tracks it is possible, over an extended timespan, to significantly improve their orbit

**Table 3** Recent and current series of satellite altimeters. After Robinson (2010).

<i>Altimeter</i>	<i>Agency</i>	<i>Dates</i>	<i>Height</i>	<i>Orbit</i>	<i>SSHA r.m.s. accuracy</i>
TOPEX/Poseidon	NASA/CNES	1992–2005	1,336 km	9.92 day repeat non–Sun-synchronous	2–3 cm
Poseidon-2 on Jason-1	NASA/CNES	2001–present	1,336 km	9.92 day repeat non–Sun-synchronous	~2 cm
Poseidon-3 on Jason-2	NOAA/ NASA/CNES Eumetsat	June 2008– present	1,336 km	9.92 day repeat non–Sun-synchronous	~2 cm
Radar altimeter on ERS-1	ESA	1991–2000	780 km	3 & 35 day repeat Sun-synchronous(RA)	~5–6 cm
RA on ERS-2	ESA	1995–2003	780 km	35 day repeat Sun-synchronous	~5–6 cm
RA2 on Envisat	ESA	2002–present	800 km	35 day repeat Sun-synchronous	3 cm
Geosat	U.S. Navy	1986–1989	800 km	17.05 day repeat Sun-synchronous	10 cm reanalysis
Geosat Follow-on	U.S. Navy	2000–present	880 km	17.05 day repeat Sun-synchronous	~10 cm

denitions by cross-referencing to the better known T/P or Jason orbits (Le Traon et al., 1995; Le Traon and Ogor, 1998). The accuracy quoted for the SSHA applies only after this procedure has been performed, and would otherwise be much worse for the ERS and Geosat families. The specification of errors for an altimeter must be handled with care because the error magnitude relates very much to the time and spacescale over which it is being averaged. The lower error attached to larger scale/longer period averaging must be set against the lesser utility of the averaged SSHA eld, especially in the context of operational oceanography.

The data products from altimeters are presented rst as along-track values of SSHA, wind speed (determined from the peak height of the echo), and significant wave height (from the pulse shape). These level 2 products are sampled every second along track, and are contained in the Geophysical Data Record (GDR), which also includes ancillary information about the various corrections applied. Whilst each agency publishes the GDR for their own altimeter, scientific users of the data may find it most helpful to work with data where cross-referencing

between different altimeters has been performed in a consistent way, referred to as the Data Unification and Combination System (DUACS), ensuring that there should be little if any bias between the SSHA from different satellites.

Data are also resampled onto a  $1/3^\circ 1/3^\circ$  Mercator grid, integrated over a period of time that relates to the orbit repeat interval. Details of these vary between the different agencies producing products.

### *Variable currents from sea surface height anomaly*

To determine an estimate of the time-variable part of ocean surface currents, geostrophic equations are used:

$$fv = g \frac{\partial h_{SSHA}}{\partial x}$$

$$fu = -g \frac{\partial h_{SSHA}}{\partial y}, \quad (7)$$

where  $(u, v)$  are the east and north components of geostrophic velocity;  $f$  is the Coriolis parameter;  $g$  is the acceleration due to gravity; and  $x$  and  $y$  are distances in the east and north direction, respectively.

From a single overpass, only the component of current in a direction across the altimeter track can be determined, but where ascending and descending tracks cross each other the full vector velocity can be estimated. Because Equation (7) assumes geostrophic balance, if there is any ageostrophic surface displacement it will lead to errors in  $(u, v)$ . However, ageostrophic currents should not persist for longer than half a pendulum day ( $1/f$ ) before adjusting to geostrophy. Thus the spatially and temporally averaged SSHA maps produced from all the tracks acquired during a single repeat cycle (10, 17, or 35 days depending on the altimeter) should represent a good approximation to a geostrophic surface that can be inverted to produce surface geostrophic currents. Close to the Equator the SSHA cannot be interpreted directly in terms of surface currents since here  $f$  is very small and the geostrophic equations (7) cannot be applied.

### *New altimeter data products*

In the relatively near future it is hoped that the lack of knowledge about the geoid can be remedied. What is needed is a means of measuring without using

altimetry, and this is provided by measurement of the gravity field above the Earth from satellites. Both the presently operating Gravity Recovery And Climate Experiment (GRACE) and the Gravity and Ocean Circulation Explorer (GOCE) mission which was launched in mid-2009 measure elements of the gravity field from which it is possible to recreate the sea level geoid. At the required accuracy of about 1 cm GRACE can achieve this only at a lengthscale longer than several hundred kilometers, but it is hoped that GOCE can do so once and for all down to a length-scale of about 100 km. This will allow steady-state ocean currents to be derived from archived altimetric data and greatly improve the capacity to utilize altimetric data in near-real time.

In anticipation of the eventual availability of a high-quality, independent geoid from GOCE, a hybrid mean dynamic topography (MDT) was produced (Rio and Hernandez, 2004) using the following approach. The absolute dynamic topography of the sea surface,  $h_{dyn}$ , is the sum of the SSHA and MDT. Eventually MDT should be determined precisely by subtracting an independent measure of  $h_{geoid}$  from MSS. This was done approximately using the EIGEN-GRACE03S geoid, evaluated to spherical harmonic degree 30, which implies that it contains little useful information on geoid variability at lengths less than 400 km but is quite well defined for length-scales above 660 km. To improve the accuracy of MDT at shorter lengthscales it was tied to the dynamic height associated with in situ measurements of steady currents using an inverse technique. The in situ data were buoy velocities from the WOCE–TOGA program, corrected for mesoscale variability using coincident SSHA. Comparison with independent velocity observations show differences to be globally less than 13 cm/s r.m.s. From MDT a new altimetry product is produced called the absolute dynamic topography ( $ADT=MDT+SSHA$ ) from which absolute currents can be estimated using standard geostrophic retrieval, following Equation (7) with  $h_{ADT}$  replacing  $h_{SSHA}$ .

### *Measuring significant wave height from altimeters*

When an altimeter measures the time for an emitted pulse to return, it tracks in detail the shape of the leading edge of the echo, from which it is possible to make a very good estimate of significant wave height,  $H_{1/3}$ , within the pulse-limited footprint illuminated by the altimeter. For a perfectly flat, calm surface the return echo has a very sharp edge. If there are large waves, several meters in height from trough to crest, then the return signal starts to rise earlier, as the first echoes are received from the crests, but takes longer to reach its maximum,

when the first echoes are received from the wave troughs. The rising edge of the echo is modeled by a function in terms of the root mean square ocean wave height, so that by matching the observed shape to the model function it is easy to gain an estimate of  $H_{1/3}$ . This method has delivered robustly accurate measurements of  $H_{1/3}$  for more than 20 years from different altimeters (Cotton and Carter, 1994) and comparison with buoys shows root mean square differences of only 0.3 m (Gower, 1996), which is the limit of buoy accuracy.

## Scatterometers

A scatterometer is the simplest type of radar used for remote sensing. It is an oblique-viewing radar pointed towards the sea from aircraft or satellites at incidence angles normally between  $20^\circ$  and  $70^\circ$ . The receiver simply measures the backscattered power from the field of view in order to determine  $\sigma_0$ . There is no attempt to preserve phase information after demodulation of the microwave signal. Therefore it does not resolve variations of  $\sigma_0$  in range or azimuth in a detailed way and cannot generate a high-resolution image. By measuring the average  $\sigma_0$  over a wide area of sea (with a spatial resolution typically 20–50 km) it uses this to estimate the wind speed.

The interpretation of scatterometer measurements of backscatter relies on an empirically derived model of the relationship between  $\sigma_0$ , wind speed, incidence angle, and the direction of the wind relative to the radar azimuth. As long as at each point on the ground is measured at least twice in close succession (see Fig. 24), viewing from different directions, there is in principle enough information to be able to retrieve an estimate of wind speed and direction using this model. The greatest uncertainty for measuring the wind speed with scatterometer is when the wind speeds are low, since the backscatter signal is weak leading to the relatively high noise, and also the direction of low winds tends to be spatially variable. However, errors in measuring low winds are generally of less importance for meteorological and oceanographic applications. The problem with measuring high winds lies in the difficulty of obtaining the in situ measurements that are needed to ensure that the wind modulation functions are accurately defined in high wind regimes.

So far, scatterometers have become accepted as operational instruments, used by meteorologists as a source of real time information on global wind distribution and invaluable for monitoring the evolution of tropical cyclones and hurricanes. Oceanographers also have come to rely on the scatterometer record for forcing ocean models. Scatterometers deployed to provide operational meteorological

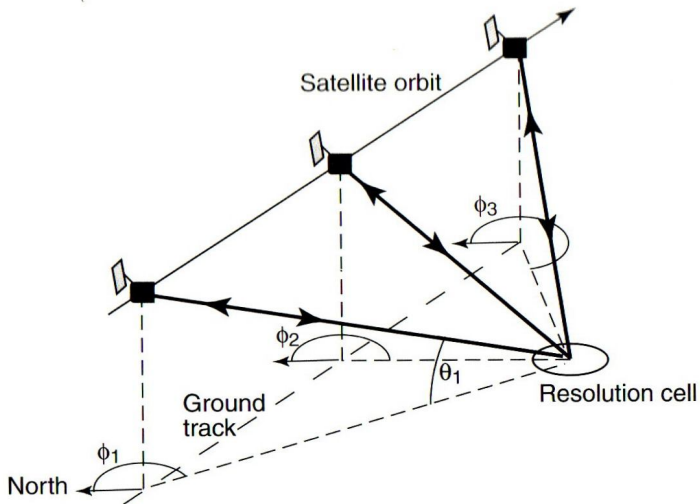


Figure 24. The multiple-azimuth viewing of a scatterometer. After Robinson (2010).

measurements have swaths spanning about 1,500 km and can view the global ocean surface twice in two days. As operational systems are developed for ocean forecasting they will look to scatterometers to provide near-real time input in, for example, oil spill dispersion models or wave forecasting models. An example of near-surface wind field map for the NE Atlantic acquired with SeaWinds scatterometer onboard QuikScat satellite for 19 July 2006 is presented on Fig. 25.

### Imaging radars

With an active device, there is scope to measure not only the energy ux of the reected signal, but also its detailed amplitude and phase, depending on how complex a measuring device is used, and how much data can be sampled and transmitted back to the ground station. Thus the timing of the return signal can be used to resolve between patches of sea surface at diereent distances from the radar. Moreover, the detailed shape of the return pulse can be compared with the pulse that was originally transmitted and, for example, Doppler shifts can be detected. When suitably analyzed, such information can be made to yield further information about the sea surface, and in particular to improve the spatial resolution of detection making it possible to generate detailed images of surface roughness. Instruments that collect such detailed information are known

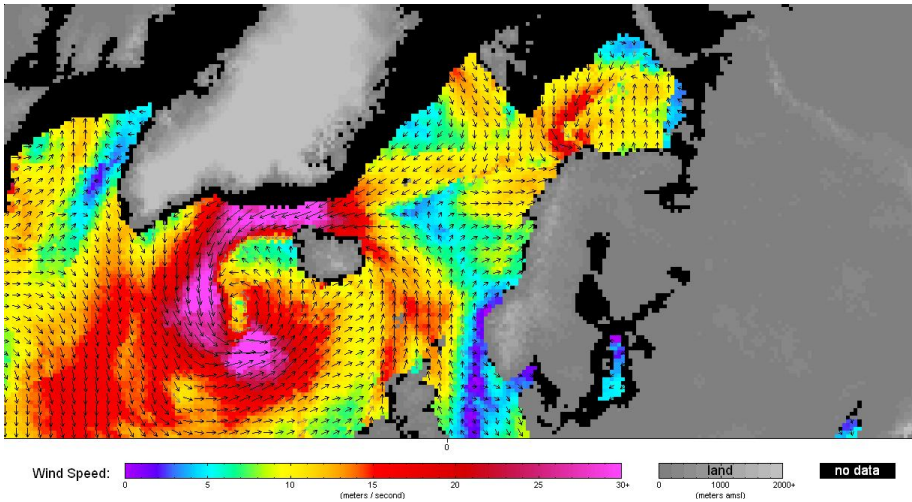


Figure 25. Near-surface winds over the NE Atlantic as measured by WindSat scatterometer for 19 July 2006. © NASA

as imaging radars. Most imaging radars on satellites belong to a class known as synthetic aperture radars (SARs) because of the way they process data to recover detailed spatial resolution in the azimuth direction.

### *Principles of SAR*

Fig. 26 illustrates the basic arrangement of a typical SAR flown on a satellite. The radar is carried on a satellite in low earth orbit, usually near-polar, at an altitude of between 600 and 800km. It has quite a large rectangular antenna, typically 10m by 1m, the long dimension being aligned with the orbit track so that the radar beam is sent out to the side of the satellite, normally with its axis at  $90^\circ$  to the direction of travel. The beam from an antenna of such a shape will spread out vertically more than it does horizontally. Since the beam axis is tilted towards the ground with an incidence angle of between  $15^\circ$  and  $60^\circ$ , the beam footprint widens with distance away from the radar. Pulses are emitted and the echo, the microwave energy backscattered from the sea surface, is detected by the antenna like any other radar.

What makes this different from a scatterometer is firstly the type of pulse emitted and then the fact that it receives and records the echoes coherently, requiring a detector with very high sampling rate and a high capacity data system. Coherent recording of the echoes enables the phase history of individual



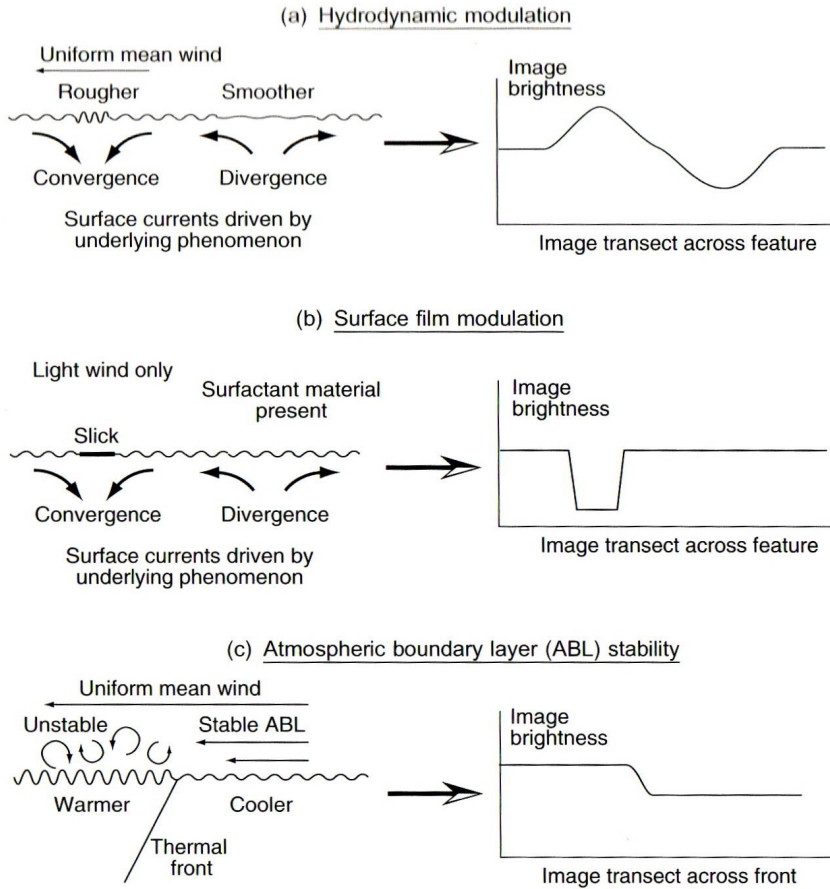


Figure 27. Processes by which an underlying ocean phenomenon modulates the radar-measured roughness to produce a signature on a radar image. After Robinson (2010).

dark patches on the SAR image can be interpreted as convergent and divergent regions. Their spatial distribution outlines the horizontal structure of the underlying ocean process that produces the current field. Driven by phenomena such as long-surface swell waves, internal waves, flow over undulating shallow topography, or ocean fronts and eddies, the hydrodynamic interaction between variable surface currents and the energy of Bragg ripples is able to generate signatures in the  $\sigma_0$  field.

The second mechanism is *surface film modulation*, also driven by the converging and diverging surface current field, but in this case acting on material

at the surface such as mineral oil or naturally occurring organic film. Convergent surface currents draw the surface material into a thicker film which reinforces the damping effect and cause the image to be darker. Divergent currents cause the surface films to be thinner and less able to damp the surface, but there is little effect on the image since this mechanism can never make the surface rougher than the natural equilibrium with the wind, as happens with hydrodynamic modulation.

The third mechanism occurs when changes in sea surface temperature (SST) affect the *stability of the atmospheric boundary layer* (ABL). In a uniform wind field the SAR backscatter might be expected to be uniform. In conditions where the ABL is neutrally stable over warmer, there will be a tendency for it to become more stable when it encounters a colder SST e.g. during the upwelling. The stable ABL produces lower surface roughness for the same mean wind speed, and hence the SAR records a weaker backscatter over the colder water. In the optimum conditions the SAR image can reveal quite clearly the front between cooler and warmer SST as a boundary between otherwise uniform fields of weaker and stronger backscatter (darker and lighter regions on the image). Example of SAR imaging of cold coastal upwelling front having clear signatures in MODIS SST image is shown on Fig. 28.

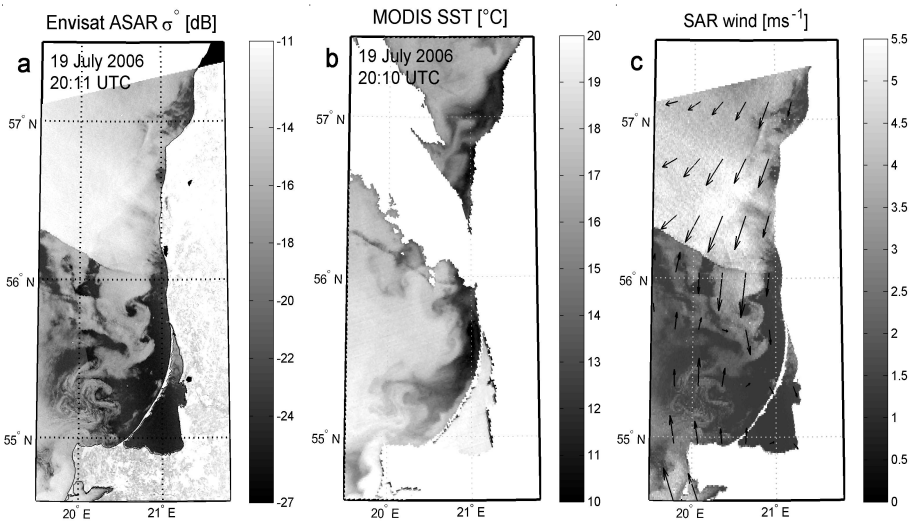


Figure 28. Example of Envisat ASAR imaging cold coastal upwelling front in the SE Baltic on 19 July 2006. (a) Envisat ASAR radar backscatter image [dB], (b) MODIS Terra SST map and (c) SAR derived near surface wind speed. © ESA © NASA. After Kozlov *et al.* (2012).

In this example cold upwelling front have SST drop about 5-7°C (Fig. 28, b). On the SAR image the cold frontal zone is manifested as dark area (Fig. 28, a), meaning that the radar backscatter is low here due to the atmospheric stability increase over upwelling zone and consequent decrease of turbulence regime and hence the near-surface wind speed (Kozlov et al., 2012) (Fig. 28, c). Remarkable that unlike the SST data affected by clouds (upper part of the SST image), under the moderate winds the SAR image provides not very strong but still valuable manifestation of the thermal front location. Thus processes whose center of action may be tens of meters below the sea surface are painted on the radar images, providing an unexpected opportunity to gain new scientific understanding of subsurface phenomena. As the surface wind is the primary phenomenon influencing the SAR image intensities, its retrieval from the high resolution SAR data is an important geophysical products available from imaging radars. Fig. 29 shows an example of initial radar image taken with Advanced SAR (ASAR) onboard ENVISAT satellite over the Southern Baltic Sea on 26 December 2009 (Fig. 29, a) and

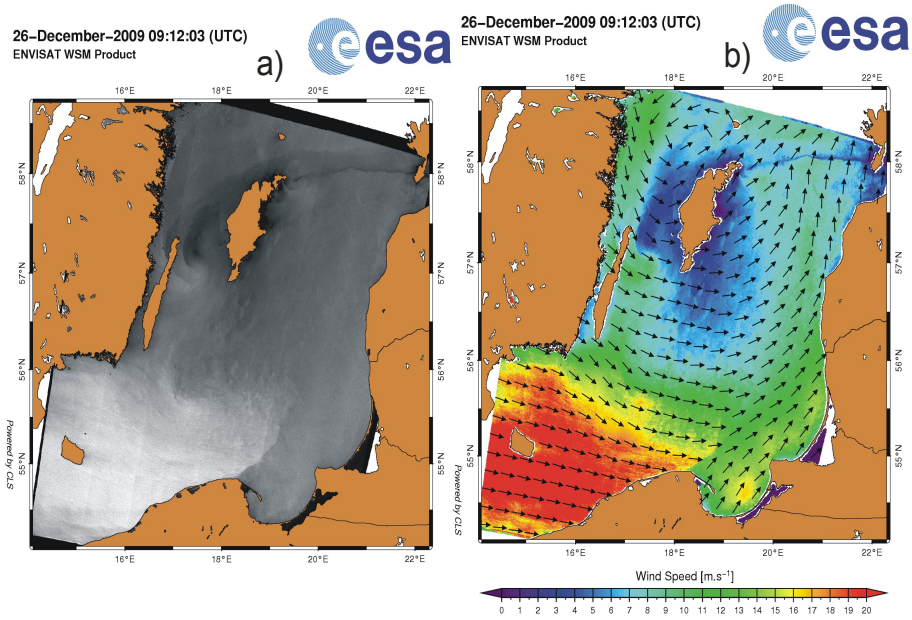


Figure 29. High-resolution wind speed mapping from SAR images. a) Initial Envisat ASAR image acquired over the Southern Baltic Sea on 26 December 2009, b) near-surface wind speed map calculated from ASAR image in a) using CMOD-2 IFR empirical function and wind direction from ECMWF model.

corresponding high-resolution wind speed map calculated from that ASAR image using CMOD-2 IFR empirical model and wind direction from ECMWF model. As seen from Fig. 29 SAR image indeed provides a unique and spatially-detailed map of near-surface wind speed depicting atmospheric fronts and mesoscale wind variability in the open sea and coastal areas.

**PART II**  
**PRACTICAL ASSIGNMENTS FOR THE MASTER PROGRAMME**  
**COURSE “REMOTE SENSING IN OCEANOGRAPHY”**

Practical assignment No.1:

***Determination of Chlorophyll “a” Concentrations According  
to the Satellite Remote Sensing Data***

*Objectives:* to define the regions of chlorophyll “a” maximum concentration for a given period according to the satellite remote sensing data, and to compare with the literature data sources.

*General explanations:*

The study of the ocean color is related to the visual observations of the Earth using the visible light spectrum of electromagnetic waves. The disadvantage of observations in the visible light spectrum is the possibility to implement them in the daylight only and the impossibility to observe the Earth in cloudy conditions. Therefore, observations of ocean color are possible in cloud-free conditions only (Fig. 30).

While performing spectrometer measurements in the visible range, the main measurable parameter is the chlorophyll “a” concentration, which, in turn, to a first approximation, is proportional to the phytoplankton concentration [6]. Light absorption by phytoplankton pigments (chlorophyll “a”, pheophytin) determines the spectral content of radiation coming from the sea, by measuring of which the absorbing pigments concentration can be calculated, and hence it is possible to evaluate the concentration of phytoplankton. However, the direct measurements of the spectral composition of radiation coming from the sea cannot be performed due

to light scattering in the atmosphere, which is carried out by the molecules of gases being part of the air, and by various aerosols. To take atmospheric influence into account, “the atmospheric correction” is to be introduced.



Figure 30. Cyanobacteria Bloom in the  
Baltic Sea, July 24, 2003

The history of the ocean color studies started from the launch of the satellite Nimbus-7 with a sea color scanner CZCS (Coastal Zone Color Scanner). The CZCS scanner provided data on the ocean color from 1978 to 1986 in 6 channels of visible and near infrared subspectrum with a resolution of about 1 km. At the Miami University and at the Goddard Space Flight Center of NASA the methods of the phytoplankton concentration global and regional maps creation were developed according to the data of such a survey. As a result, the atlas “Ocean Color from Space” was created [Ocean Color from Space. NSF-NASA-sponsored US Global Ocean Flux Study Office. Woods Hole Oceanographic Institution, 1989.], wherein the global and regional diachronic maps of the ocean color are collected specifying the distribution of the chlorophyll concentration in different regions of the World ocean.

Ten years later the data on the ocean color started to come once again being available due to MOS sensors mounted on the IRS P3 satellite (India), OCTS and POLDER on the ADEOS satellite (Japan) in 1996: and from August, 1997, the SeaWiFS spectroradiometer (Sea-viewing Wide Field-of-view Sensor) on the OrbView-2 satellite or as it is called more often – Seastar (it transmitted information until December, 2010) began providing with such pictures on a regular basis.

Already on December 18, 1999 and on May 4, 2002, the EOS AM-1 (Terra) and the EOS PM-1 (Aqua) satellites were correspondingly launched with MODIS spectroradiometers (MODERate-Resolution Imaging Spectroradiometer). They have been transmitting information until present. The technical capabilities of these satellites allow scanning each square kilometer of the ocean every 48 hours, which gives an opportunity to monitor the ocean surface under the condition of the dense atmospheric clouds absence. In March, 2002, a satellite of the European Space Agency with the MERIS spectrometer (MEDIum Resolution Imaging Spectrometer) was launched. But it operated up to April, 2012.

On the website of the international consulting team for the ocean color study <http://www.ioccg.org/sensors/current.html> you will find a list of spectroradiometers currently transmitting information about the ocean color as well as the specifications of all operated and operating scanners ([http://www.ioccg.org/sensors\\_ioccg.html](http://www.ioccg.org/sensors_ioccg.html)).

One of the major research programs for the ocean color is a NASA’s program referred to as the Ocean Color (<http://oceancolor.gsfc.nasa.gov/>), and which is supported by several other projects and centres: Distribute Active Archive Center (DAAC), Data and Information Services Center (DISC), Goddard Earth Sciences (GES). At present, the Ocean Color provides access to different data

among which the data of the SeaWiFS and of the MODIS should be distinguished. They have the longest duration of measurements and the finest area resolution.

A work with the ocean color data may be divided into 2 types by the level of complexity, by the volume of necessary knowledge and by the technical equipment available.

The simplest, but in some cases, sufficient method is the processing of ready-to-use data on the chlorophyll “a” concentration. Such data are available at <http://oceancolor.gsfc.nasa.gov/cgi/l3>. These are the data of the so-called 3<sup>rd</sup> level (level 3). The resolution of the SeaWiFS data is 4096 by 2048 pixels (a spatial step is about 9 km). The MODIS data have just the same or higher resolution of 8640 by 4320 pixels (a spatial step is about 4 km). The data are accessible in the PNG graphic format or in the HDF binary one. To evaluate in a qualitative manner the time-space variability of chlorophyll “a” fields, it makes sense to take advantage of the pictures in the PNG-format, and to evaluate it in a quantitative manner – in the HDF binary format. These data have two substantial defects: they are not in a finest resolution and they do not take into account the regional peculiarities of the sea water, which makes the use of these data for the sea waters of the gulfs and of the coastal regions (so-called the second class waters) highly questionable. The data are ideally suitable for the studies of chlorophyll distribution in the mid-ocean waters (the first class waters), in the composition of the upwelling radiation thereof phytoplankton pigments make the main contribution.

Fig. 31 Average Perennial Field of Chlorophyll Concentration in March.

A work with “raw” data received from each channel of the spectrometer is the more complicated version of the ocean color data analysis. That allows developing (where synchronous subsatellite data are available) of so-called regional algorithms for the simultaneous recovery of the chlorophyll “a” concentration, of the mineral suspended matter and of the dissolved organic matter [8].

The study of the chlorophyll global distribution in the World Ocean becomes possible due to the creation of composite maps which are created by layering multiple images. Thus, the gaps arising from the clouds on each individual picture are filled in. In case when the same pixel of data is available on two different images, the newest information is to be saved. In this way 3-day and 8-day maps appear. Those reveal the peculiarities of the global phytoplankton distribution: in coastal regions, especially in areas of permanent upwellings, and advancing into the higher latitudes, one can observe the increase of phytoplankton content.

Fishery is a practical application for chlorophyll concentration data. Data on Chlorophyll in conjunction with altimetry and sea surface temperature (SST) data are used for selecting areas for fishery. It is explained by the fact that phytoplankton abundance results in zooplankton abundance eating it, which in its turn attracts fish fed on zooplankton. Therefore the presence of high concentrations of phytoplankton defined by the ocean color stands as an indicator of fish potential presence [3, 4].

Apart from the fishery, information on chlorophyll “a” concentration, mineral suspension and dissolved organic substance is used for evaluating the water quality of basins allowing tracking both the time and the space variability. As an example, the average perennial field of the chlorophyll concentration in the Baltic Sea for March is shown on Fig. 31. It can be used as a basis for evaluating the anomalies of chlorophyll content in different years [1, 2]

Information from the above satellites can be obtained using several methods. Sometimes it is necessary to become an authorized user to have an opportunity to upload raw digital information from various ftp-servers or to order it on the

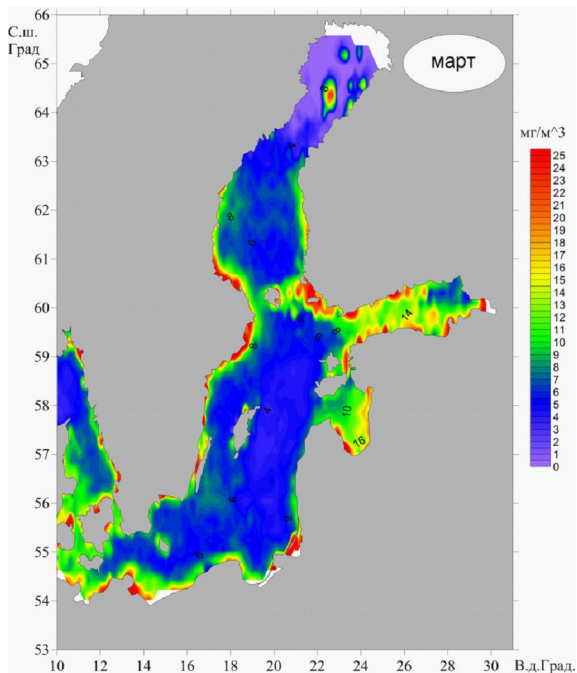


Figure 31. Average Perennial Field of Chlorophyll Concentration in March.



medium. All this is for the non-commercial use only and it can be used on the condition that the source of used information has to be cited in any publication. If you have a task to obtain an image and data of high quality not for the entire globe, but for a particular region, then you can use the following link: <http://seawifs.gsfc.nasa.gov/cgi/browse.pl?typ=GAC> (Fig. 32), wherein there is an opportunity to enter the coordinates of the area of interest or to choose one of the proposed areas. The search will result in the set of track images and links to the “raw” data of the first and the second level (GAC) in the HDF format, which contain some predetermined areas of the ocean. To work with HDF files there are various programs but we recommend to use the SeaDAS specialized package (<http://seadas.gsfc.nasa.gov/>), allowing handling the data both by the standard algorithms and giving an opportunity to use the regional algorithms. Until a few years ago to work with SeaDAS required knowledge and experience with operating systems based on UNIX, now an installation of SeaDAS under Windows as well as for MAC computer is possible. But we must be prepared to the fact that initial information has a large volume and will require rather a lot of space on the hard disk of your computer, if you want to determine a long-term database of satellite data on chlorophyll.

The website of Colorado Center for Astrodynamics Research [http://eddy.colorado.edu/ccar/ssh/nrt\\_global\\_grid\\_viewer](http://eddy.colorado.edu/ccar/ssh/nrt_global_grid_viewer) can serve as an alternative, on which the convenient support for output chlorophyll fields maps for the regions with fixed coordinates is provided and an opportunity of combining these maps (or SST) with the data on the SSH (Sea Surface Height) altimetry is suggested.

For those who are familiar with the data in the NC format the website <http://hermes.acri.fr/GlobColour/> will be more convenient. The advantages of \*.nc are in its compactness and opening convenience. There are several file viewers of this format, but we recommend you to use MatLab when data processing, which already has the support of this format. The data of SeaWiFS, of MODIS and of MERIS are accessible: both on chlorophyll and on individual channels. The website gives an opportunity to select the resolution at which you want to obtain the data (4, 25 or 100 km), their discreteness (1 day, 8 days, a month) and a time period (Fig. 33). To select data for the region you are interested in, please do highlight the relevant area on the map or enter its coordinates. Then you have to click the “Search” button. In a few seconds a window with a list of files found will appear. Click the “Order Products”. A message with the order confirmation and an e-mail enquiry will appear. Enter your e-mail and visit the mailbox to finish enquire the data. In the message you have received please

confirm the data order. After that, you will receive an inbox message with a password to the ftp server wherefrom you will be able to download all the data you have enquired. After uploading the data, you will get a database on chlorophyll for the specified period of time and for the selected area.

Details on the data, methods of their preparation will be found in the “Product User Guide” available on the link at the top right of the website.

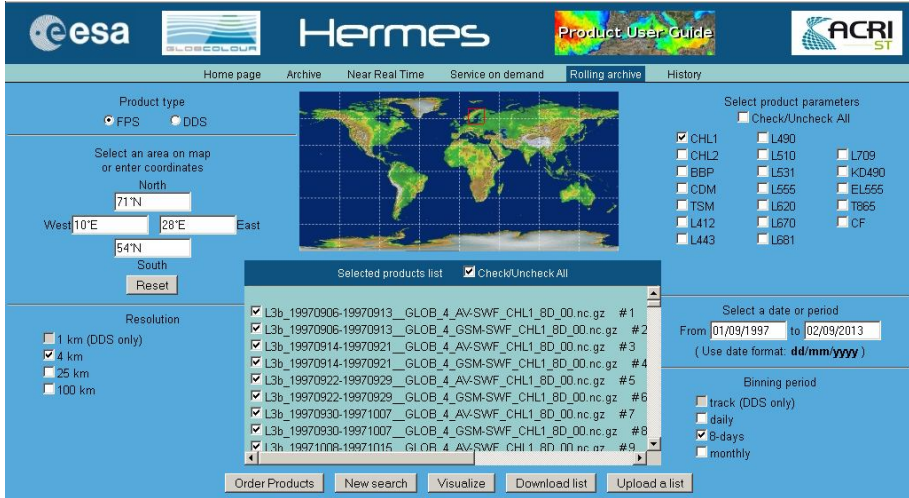


Figure 33. The interface for the online-order of third type data on Chlorophyll (L3).

The links hereto were operable within the period of these materials preparation. For more details we can recommend [10] for reading in Russian and [11] – in English.

### *Methodology of the work*

Download the maps of the Baltic Sea color for the period specified by a teacher from any of these sources, perform the analysis of them to identify the areas and the periods of chlorophyll “a” maximum concentration. References describing the specified period to be selected by yourself, and the results obtained to be compared.

### *Initial data*

- The archives of the satellite images of the Baltic Sea in the visible light from any of the sources.
- References.

## *Report Preparation*

The report must include maps of sea water color for the specified period, an analysis of the bloom areas distribution on the basis of satellite images, a comparison with literature data, conclusions, and a list of references used.

### *Recommended reading*

1. Gusev A.K. Zakharchuk E.A. Klevantsov Y.P. Smirnov K.G. Tikhonov N. A. Large-scale variability of oceanographic characteristics fields in the Baltic Sea according to satellite measurements//the monograph “Complex Research of Processes, Characteristics and Resources of the Russian Seas of the North European Region” - the draft of the subprogramme “Research of the World Ocean nature “, FTP “World Ocean”, Iss. 2 . Apatity. 2007.
2. Watson W. Gregg, Margarita E. Conkright, Paul Ginoux, John E. O'Reilly, Nancy W. Casey. Ocean primary production and climate: Global decadal changes // GEOPHYSICAL RESEARCH LETTERS, VOL. 30, NO. 15, 1809, doi: 10.1029/2003GL016889, 2003.
3. T.V.Belonenko, E.A.Zakharchuk, A.V.Koldunov, K.G.Smirnov, D.K.Staritsin, N.A.Tikhonov, V. R. Fucks. Experience of satellite information use for an assessment and the forecast of biological and fishery efficiency of various World Ocean regions //Questions of Fishery Oceanology. Iss. 7 . No 1. Moscow: VNIRO prod. 2010. 206-225pp.
4. Fucks V. R., Belonenko T.V. Problems of use of satellite information for chlorophyll concentration for biotic conditions of feeding fish catch assessment//Questions of trade oceanology. iss. 3 . No 3. Moscow: Prod. VNIRO. 2006. 241-263pp.
5. Kahru M., Savchuk O.P., Elmgren R. Satellite measurements of cyanobacterial bloom frequency in the Baltic Sea: interannual and spatial variability // MARINE ECOLOGY PROGRESS SERIES, Vol. 343: 15-23, 2007.
6. Finenko Z.Z. Shemshura V. E. Bourlakov Z.P. Assessment of superficial chlorophyll-a concentration on the effective ascending radiation wavelength // Oceanology. 1990 . T. 30 . No. 5. Page 827-833
7. Interactive tutorial “Fundamentals of remote sensing” by Canada Centre for Remote Sensing ([http://www.nrcan.gc.ca/sites/www.nrcan.gc.ca.earth-sciences/files/pdf/resource/tutor/fundam/pdf/fundamentals\\_e.pdf](http://www.nrcan.gc.ca/sites/www.nrcan.gc.ca.earth-sciences/files/pdf/resource/tutor/fundam/pdf/fundamentals_e.pdf))
8. Korosov A.A. Pozdnyakov D. V. Assessment of a condition and tendency of primary production change in the White Sea according to remote sensing for

the last five years: methods and first results//Problems of studying, rational use and protection of resources of the White Sea. Materila IX of the international conference. Petrozavodsk. 2005.

9. Pozdnyakov D.V. and Grassl H. 2003. Colour of inland and coastal waters: A methodology for its interpretation, Chichester: Springer-Praxis.

10. Kashkin V.B., Sukhinin A.I. Remote sensing of Earth from space. Digital processing of images: Manual. M: Lagos. 2001. 264 pages.

11. Seelye Martin. An introduction to Ocean Remote Sensing. Cambridge University Press. 2004.

12. Ocean Biology Processing Group; "SeaDAS Training Manual," 29 October 2007 (electronic [http://seadas.gsfc.nasa.gov/seadas/seadas64/SeaDAS\\_Training/SeaDAS\\_Training\\_Manual.pdf](http://seadas.gsfc.nasa.gov/seadas/seadas64/SeaDAS_Training/SeaDAS_Training_Manual.pdf))

## **Practical assignment No. 2:**

### ***Determination of Sea Surface Temperature According to Remote Sensing Data***

*Objectives:* To obtain a sea surface temperature variability diagram along the transect

*General explanations:*

Waters temperature plays a key role in the formation of currents, it is one of the parameters of the ocean state and defines the conditions of living environment. With that, the waters of the surface layer are most densely populated by living creatures and are of the most interest for mankind from a practical standpoint. For instance, the development of surface temperature distribution maps is necessary for successful work of the fishery industry. Besides, the waters of the World Ocean are able to accumulate, to transfer and to radiate heat which directly influences the heat reserve of the atmosphere. Thus, the surface temperature distribution data are necessary for creating weather forecasts and for evaluating the climate. The present services successfully decipher satellite infrared images and provide temperature distribution maps for commercial and scientific purposes. [13]

As was mentioned above, infrared or, sometimes, microwave radiation bands are used to measure surface temperatures. With that, the radiation of the 1 mm upper layer called a skin-layer is registered. An obtained signal is transferred to the data processing center wherein corrections for atmospheric radiation are carried out and other corrections are introduced, and the geographic coordinates location is performed. The values of received radiation are called a

“radiance temperature”, which are grey pixels of different shades on an image. For users convenience the signal intensity is broken into bands for a brighter contrast, or a color scheme is used. Since it is impossible to receive an infrared signal from the sea surface through the cloud covered skies, the water area maps covered with clouds are collected from several successive overlapping satellite images constituting a composite image. The traces of moisture in the atmosphere and the location of clouds reflect a synoptic situation on large areas. To compensate for the atmosphere vapours effects, various parameters are used, such as surface temperature at weak winds or sea surface temperature in the conditions of the upper layer uniformly stirred over. Before the use of any dataset the verification of the accuracy in temperature measurements from satellites requires in-situ measurements.

### *Methodology of the work*

Select appropriate maps from the archives of the satellite data on the sea surface temperature, which are relevant to the period mentioned by the teacher, draw up a temperature map and mark a prescribed transect on it, then plot a graph of temperature variability along the transect, and analyze the obtained results.

### *Initial data*

The archives of the satellite images of the Baltic Sea surface temperature from the sources mentioned in the introduction.

### *Report Preparation*

The report should contain a map of sea surface temperature distribution with a transect marked on it, a chart of temperature variability along the transect, and an analysis of the results obtained.

### *Recommended reading*

13. GHRSSST Science Team (2010), The Recommended GHRSSST Data Specification (GDS) 2.0, document revision 4, available from the GHRSSST International Project Office, 2011, pp 123.

14. Seas of the USSR project. Hydrometeorology and hydrochemistry of the seas of the USSR. Volume III Baltic Sea. Release of I. Hydrometeorological

conditions. / Under F.S.Terziyev, V.A.Rozhkova, A.I.Smirnova's edition. – SPb. Gidrometeoizdat, 1992.

15. Group for High Resolution Sea Surface Temperature GHRSSST: <https://www.ghrsst.org/ghrsst-science/science-team-groups/stval-wg/>

### **Practical assignment No.3:**

#### ***Determination of Sea Level Variability According to Satellite Altimeters Data***

*Objectives:* Calculation of sea level variability statistical evaluations according to the data obtained by the Jason-1 and the Jason-2 satellites.

*General explanations:* Map of Subsatellite tracks for the Jason-1 and Jason-2 altimeters.

Opportunities to study the sea level variability were limited by coastal measurements for a long period. Therefore, there are long series of high resolution measurements on monitoring posts; however, series of measurements in the open areas of the World Ocean are rare and short, which is connected with difficult access to the open regions of the sea and with the high price of applicable equipment. The emergence of technologies and altimetry measurement devices onboard satellites has given an opportunity to obtain data on the sea level beyond coastal posts on a regular basis [16].

The products of satellite altimetry possess a great potential for the sea dynamics study. The satellites meant for resolving oceanographic objectives are track repetitive, i.e. allowing conducting regular measurements along the orbit and accumulating series of data for specific points along the Earth track (Fig.34). Data obtained by satellite altimeters can be considered from the two points of view. First, subsatellite tracks represent quasi-instantaneous measurements on a large water area and they can give an idea about the horizontal scopes of level fluctuation. Whereas regular measurements allow accumulating series of level values in the specific points of the water area with an accuracy of up to the fourth digit by longitude and by latitude.

The history of the underlying surface altitude measurements started from the early 70-ies of the XX century. The first data obtained from the Skylab-IV, the GEOS-3 and the SEASAT satellites showed a possibility in principle to use satellite altimeters in scientific purposes and for the monitoring. However, only since 1993, when the ERS 1/2, the TOPEX/Poseidon, the GFO-1, the Jason 1/2, the Envisat, etc. were launched, the new phase of altimeters usage for oceanology commenced.

Currently, the most attention has been paid to data from the Envisat, the Jason-1 and the Jason-2 satellites due to these satellites accuracy and operational lifetime. Altimeters data from these carriers have passed intercalibration and occurred within the last decade. Their surface deviation measurement level of accuracy is about 2 centimeters. Unfortunately, the Envisat stopped transmitting data in April, 2013, and the Jason-1 was transferred to a new orbit in 2008. Great expectations are associated with the operation of the new satellite Cryosat-2 which was put into operation in February, 2012. The joint altimetry measurements from these satellites can supply information on the dynamics of sea level change on the background of climate change within the last decade. In the coming years it is planned to launch some more satellites, for instance the Jason-3, the SWOT (Surface Water and Ocean Topography). Altimeters data contain information on coordinates and measurement time, delay, and capacity and shape of the reflected pulse. The primary processing allows getting the values of distance from the altimeter to the underlying surface on the basis of the orbit forecast, excluding the measurements carried out above the land, evaluating the quality of information obtained and converting it to a format convenient for storage and use. Such processing is carried out by the Space Oceanography Division CLS in France (Collecte Localisation Satel-

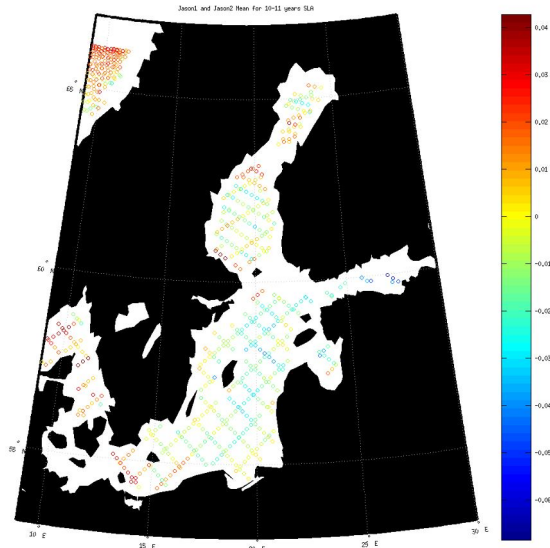


Figure 34. Map of Subsatellite tracks for the Jason-1 and Jason-2 altimeters

lites Space Oceanography Division). Processing takes 3 to 9 hours and assumes the operational use of information. The data of this type can be found on a data server in the OGDR section – Operational Geophysical Data Records. For a more accurate calculation of the distance from the sea surface to the altimeter receiver, it is necessary to consider a number of amendments. The corrections can be conditionally divided into instrumental, atmospheric and geophysical. Instrumental corrections are taken into account at the primary processing and they consider the parameters of specific altimeters and, at the intermediate data processing, the correction of the carriers orbit is taken into account on the basis of the data of the satellite itself, which increases by several times the measurement accuracy. Atmospheric corrections consider the properties of the atmosphere: dissipation directly by gases being part of the atmosphere, steam dissipation and pulse dissipation by free ions and electrons in the upper strata of the atmosphere. The refined data are introduced into the IGDR database – Interim Data Records in 1-2 weeks after the direct measurement. These data can be used for oceanographic purposes.

However, the most accurate data are the GDR – Geophysical Data Records, which are subject to the detailed processing with account of all corrections including the fact that the satellite orbit and the atmosphere state are specified once again. These data are supplied into the database with a considerable delay but they are defined by an accuracy of up to 2 cm. In the GDR archives there are data with respect to geophysical corrections and without the latter. Geophysical corrections reflect the influence of natural processes on the sea surface elevation, namely: the inverse barometer correction takes the atmosphere baric impact into account. It is calculated via atmospheric pressure at the underlying surface level  $P_s$  (mbar) as  $dh_{inv} = 9.948 (P_s - P_0)$ , where  $P_0 = 1013.3$  mbar – normal atmospheric pressure relative to the ocean undisturbed surface. The value of this amendment may reach 3 m. Besides, there is a correction considering the tide, which is introduced by the results of models calculation.

Data with and without consideration of geophysical corrections find their application in oceanography. The adjusted data are used for monitoring the sea level, its long-term dynamics, they are assimilated into the calculation of the dynamic models of the sea state, and are the integral characteristic of the sea level at the account of the direct dependence upon waters density, and they are used for the verification of the assessments obtained by simulation. The non-adjusted data contain a signal useful for oceanography within the range of synoptic and tidal time-scale, they allow calculating surface currents they are

also assimilated in the model of water dynamics and they are used for the verification of the latter.

The data quality is dependent to a large extent upon the considered corrections, the orbit calculation accuracy and the measuring area. Thus, a stated accuracy of  $\pm 2$  cm is correct for the open part of the sea, whereas the sea level signal in the coastal areas is corrupted due the presence of islands and shores.

As was mentioned above, the altimeter allows measuring a distance from the device to the surface, the received value is comparable to the carriers orbit altitude and constitutes 800 to 1400 km depending on the carrier and its current position at a measuring instance. This presentation is not convenient to solve oceanographic problems; therefore, sea level anomalies (SLA) along the satellites track are presented in the databases. The SLA is a level deviation from some average position of the sea surface.

The average position of the sea surface may be presented as a sea undisturbed level which imitates the geoid shape. Insofar as the true shape of the geoid is unknown, an average sea level for a certain long-term period of time is used – by the mean dynamic topography (MDT) - instead of the undisturbed level. The MDT is necessary to calculate the sea absolute level which is defined as the total of MDT+SLA. The error value may constitute 3-5 cm. The SLA data for the Baltic Sea for research purposes are provided in free access from FTTP servers: AVISO, Myocean and Ifremer for scientific purposes. With that, access is provided for both global and regional products of Sea Level Anomaly (SLA) presented for each day, as well as of mean sea level anomaly (MSLA), of absolute dynamic topography (ADT) and of mean dynamic topography (MADT) to be given with a variable averaging.

On the AVISO website for to the data access permission it is necessary to be registered and to describe in detail the range of scientific tasks for which the data are inquired. By the results of the pendency of application, a login and a keyword are sent for access to the specific products. The data are presented as archives in the NetCDF format, wherein the values, coordinates and the quality of the altimetry data are presented.

Due to the high density population and the substantial exploitation of the Baltic Sea water area and shores on the background of climate intense changes and the level expressed variability, it is necessary to regularly monitor the level both in the coastal and the central part of the sea. Calculation of statistical estimations is one of the fast and sensibly demonstrative methods of sea variability evaluation. Such parameters as an average and a standard deviation give an

idea about the intensity of the sea dynamics for the period of evaluations. To obtain statistic estimations it is convenient to use the data simultaneously from the several intercalibrated satellites, for instance the Jason-1 and the Jason-2.

### *Methodology of the work*

For this task completion it is necessary to download sea level anomaly data (SLA) for the specified period from the appropriate archives, and on their basis, with the use of accessible software, to draw up sea level anomaly maps for the fixed regions. Then the statistical evaluations: mean and standard deviation are to be determined and results to be compared for various regions. After that, calculate the average position of the sea surface based on dynamic topography. For this, it is necessary to sum the SLA average values for the fixed region together with the average position of the dynamic topography (MDT) in this region. Compare the results obtained to the data of the coastal stations and analyze them.

As software, the BRAT (Basic Radar Altimetry Toolbox) package for altimetry data processing is suggested; the User's Guide can be found on the website of the Radar Altimetry Tutorial ([http://www.altimetry.info/html/data/toolbox\\_en.html](http://www.altimetry.info/html/data/toolbox_en.html)).

### *Initial data*

- Historical data of satellite altimetry from the archives for the period specified by the teacher.
- Dynamic topography array of the Baltic Sea of the Danish Meteorological Institute DMI
- Series of level values on the coastal stations.

### *Report preparation*

The report must include the SLA maps and received statistical evaluations, a level variation diagram, and a received results analysis.

### *Recommended reading*

16. Pustovoytenko V. V. Operational oceanography: satellite altimetry – current state, prospects and problems / V. V. Pustovoytenko, A.S.Zapevalov//Mo-

dern problems of oceanology: series. – Sevastopol: MGI NAN of Ukraine, 2012. “Iss. No. 11.” 208 p.

17. Lavrova O. Yu. bone A.G. Lebedev S. A. etc. Complex satellite monitoring of the seas of Russia. M: IKI Russian Academy of Sciences, 2011. 480 pages.

18. Coastal Altimetry Vignudelli, S.; Kostianoy, A.G.; Cipollini, P.; Benveniste, J. (Eds.) 2011, XII, 566p.

19. [www.aviso.oceanobs.com/en/altimetry.html](http://www.aviso.oceanobs.com/en/altimetry.html).

20. <http://www.altimetry.info/>

21. Rio, M-H. A mean dynamic topography of the Mediterranean Sea computed from altimetric data and in-situ measurements / M.-H. Rio, P-M Poulain, A. Pascual [et al.]// Journal of Marine Systems. – 2007.- V.65. – pp. 484-508.

22. E.A.Zakharchuk, N.A.Tikhonova. Intensity of level fluctuations for coastal points of the Barents and Baltic seas in the various temporary scales. In the book “Complex Researches of Processes, Characteristics and Resources of the Russian Seas of the North European Basin”. Release 1. Russian Academy of Sciences. Ministry of Education and Science of the Russian Federation. Apatity. 2004, page 325 – 335.

#### **Practical assignment No. 4:**

##### ***Determination of Surface Streams Rates Components with the Use of Satellite Altimetry Data***

*Objectives:* Calculation of the surface current field with the use of the data from the Jason-1 and the Jason -2 satellites altimeters, and comparison to the literature data.

*General explanations:*

The satellites altimeters measure the SLA non-recurrent deviation from the 7-year-old level in a certain area at a specific location 1 time per cycle. One time in 9.96 days for the Jason-1 and the Jason-2. Thus, the SLA brings a signal about a short-term level anomaly reflecting a surface direct position, average on the area, at the expense of medium-scale phenomena, such as long waves, and of synoptic time-scale processes, as well as information on a level at the expense of a water balance and of a steric state (a eustatic level component). Dynamic topography is defined directly by the data of satellite measurements of sea surface (SLA) anomaly from the mean dynamic topography (MDT). Properly speaking, in case of satellite altimetry the sea average dynamic topography means the sea level average position for the relatively short period:

1993 to 1999. As mentioned above, within these years first regular level data were received from the satellites of several missions, as well as their mutual calibration was performed. However, there are also the other mean topographies of the World Ocean used in works, for instance, in the period from 1992 to 2002, there are ocean topographies calculated on satellites and drifters data, on the wind data and on the GRACE Gravity Model-01 developed by N. Maksimenko (IPRC) and by P. Niiler (SIO).

The sea-level signal can be interpreted as a geostrophic field for calculating the velocities of surface currents [22]. The calculation of stream components is performed based on the geostrophic approach of motion equations, as described in section 13. The geostrophic rate is defined by dynamic topography gradients (“ $h$ ” $_x$  and “ $h$ ” $_y$ ) in accordance with the following equation:

$$U_g = -\frac{g}{f} \frac{\partial h}{\partial y}; V_g = \frac{g}{f} \frac{\partial h}{\partial x}. \quad (8)$$

where  $u_g$ ,  $v_g$  – geostrophic velocities;  $g = 9.8 \text{ m/s}^2$  – the gravity acceleration;  $f = 10^{-4} \text{ s}^{-1}$  – the Coriolis parameter.

As it is known, in real conditions surface currents are essentially formed by the total of geostrophic and drifting component. According to altimetry data it is possible to calculate geostrophic surface streams [23].

The drifting component of a current velocity is defined by the wind velocity above the water surface. It is assumed that the wind contributes to the rate of drifts near the surface about 0.5% U10 (U10 – wind velocity at an altitude of 10 m) and additionally 1% U10 from Stokes drift (wave action), with that, the stream deflects to the right by 45°.

One of the methods of surface currents calculation with the use of satellite data was implemented in the Maritime Hydrophysical Institute, Sebastopol, Ukraine. GrabSataData\_Baltic takes into account the geostrophic and drifting components of currents. To calculate velocities according to satellite altimetry data, regular data on sea level anomalies on the grid with a latitude and longitude special step of  $0.125^\circ \times 0.125^\circ$  is used. Maps of surface currents calculated on the basis of satellite altimetry over the Baltic Sea are brought forward as an example (Fig. 35).

*Practical assignment:* Calculation of a surface streams field using GrabSata Data (MGI).

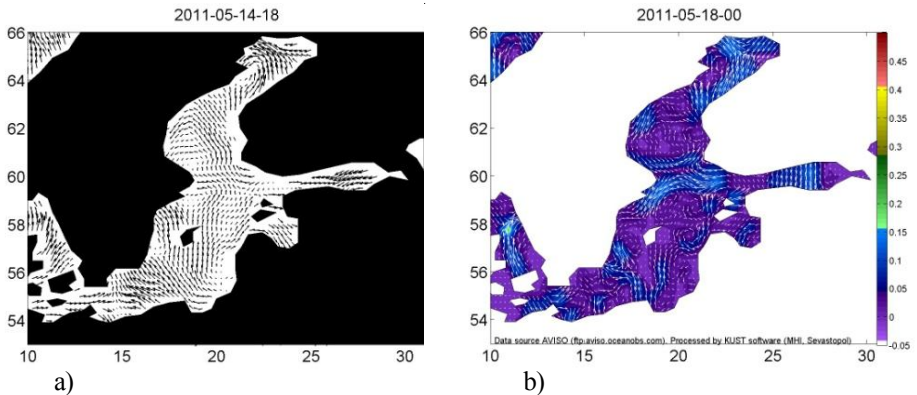


Figure 35. a) Geostrophic currents and b) currents and level .

### *Methodology of the work*

Start the program GrabSataData.exe on the computer, set the start and end time in the opened dialog box, select data of interest, press START. After finishing the program, open a directory wherein the program is installed, then open the directory Baltic which contains subdirectories dat and jpg. These directories contain the data on the variables in dat and images in jpg format respectively. In each of them there are subdirectories with the title of selected data. Analyse the results obtained.

### *Initial data and materials*

- Water bloom images from the MODIS Terra/Aqua satellite;
- Synoptic maps and surface wind maps;
- Historical data of satellite altimetry from the archives for the period specified by the teacher.
- GrabSataData.exe program.

### *Report preparation*

The report must contain information on the period, the region and the method of surface currents calculation, the level anomalies map of the Baltic Sea for the specified period, the map of surface streams for the appropriate period, the synoptic maps of surface wind, and the analysis of the results.

### *Recommended reading*

22. AA Kubryakov, SV Stanichniy, EV Plotnikov Marine Hydrophysics Institute of NAS of Ukraine, Sevastopol Determination of the surface currents velocities fields by remote sensing methods // Ecological safety of coastal and shelf areas and comprehensive utilization of resources of the shelf: a collection of scientific papers in 2011.
23. Introduction To. Physical Oceanography. Robert H. Stewart. Department of Oceanography. Texas A & M University. Copyright 2008. [http://oceanworld.tamu.edu/resources/ocng\\_textbook/PDF\\_files/book\\_pdf\\_files.html](http://oceanworld.tamu.edu/resources/ocng_textbook/PDF_files/book_pdf_files.html).
24. Rosmorduc, V., J. Benveniste, E. Bronner, S. Dinardo, O. Lauret, C. Maheu, M. Milagro, N. Picot, Radar Altimetry Tutorial, J. Benveniste and N. Picot Ed., <http://www.altimetry.info>, 2011.
25. Campbell, James B., Introduction to Remote Sensing (5th edition) 2011, Guilford.
26. Lavrova O. Yu. bone A.G. Lebedev S. A. etc. Complex satellite monitoring of the seas of Russia. M: IKI Russian Academy of Sciences, 2011. 480 pages.

## REFERENCES

1. Robinson, I. S. 2010. Discovering the ocean from space: the unique applications of satellite oceanography. Heidelberg; New York: Springer; Chichester, UK. 638 pp.
2. Robinson I. S. 2004. Measuring the Oceans from Space, The principles and methods of satellite oceanography, Springer, p. 655
3. Lavrova O. Yu. Kostyanoy A.G. Lebedev S. A. etc. Complex satellite monitoring of the seas of Russia. M: IKI Russian Academy of Sciences, 2011. 480 pages.
4. Seas of the USSR project. Hydrometeorology and hydrochemistry of the seas of the USSR. Volume III Baltic Sea. Release of I. Hydrometeorological conditions. / Under F.S.Terziyev, V.A.Rozhkova, A.I.Smirnova's edition. – SPb. Gidrometeoizdat, 1992.
5. Fu, L.-L., Satellite Altimetry and Earth Sciences. A handbook of Techniques and Applications / L.-L. Fu, A. Cazenave // International Geophysics series, Academic Press, - V.69, 2001. - 463 pp.
6. Vignudelli S., Kostianoy A.G., Cipollini P., Benveniste J. (eds.), Coastal Altimetry, Springer-Verlag Berlin Heidelberg, 578 pp, 2011. Robinson I. S. 2004. Measuring the Oceans from Space, The principles and methods of satellite oceanography, Springer, p. 655.
7. Stewart R. H. 1985. Methods of Satellite Oceanography, University of California Press, p. 360.
8. Rees W. G. 2001. Physical Principles of Remote Sensing, Cambridge University Press, p. 261.
9. Campbell J. B. 2008. Introduction to Remote Sensing, The Guilford Press, New York, p. 626
10. Ikeda M. and Dobson F. W. 1995. Oceanographic Applications of Remote Sensing, CRC Press, p. 512.
11. Ivanov V.A. Pokazeev K.V. Shreyder A.A. Oceanology bases. Sevastopol: NPTs “EKOSI-Gidrofizika”. 2005, 446c.<http://solab.rshu.ru/ru/education/>
12. Doronin YU.P. Ocean Dynamics. - Leningrad, Gidrometeoizdat, 1980, – 304 p.
13. Dobrovolsky A. Zalogin B. S. Seas of the USSR. M, Publishing house of the Moscow State University, 1982.
14. World ocean atlas 1994. Volume 3 : Salinity / S. Levitus, R. Burgett, T. P. Boyer . - NOAA ATLAS NESDIS 3, 1994. - 99 pp.

## CONTENTS

PREFACE .....	3
PART I .....	5
THEORY .....	5
Introduction .....	5
Remote sensing of marine environment .....	13
Ocean colour .....	25
Sea surface temperature measurements from thermal IR radiometry .....	30
Microwave radiometry .....	39
Radar basics. Altimetry. Scatterometry. Synthetic Aperture Radar .....	42
PART II .....	60
PRACTICAL ASSIGNMENTS FOR THE MASTER PROGRAMME COURSE “REMOTE SENSING IN OCEANOGRAPHY” .....	60
Practical assignment No.1: Determination of Chlorophyll “a” Concentrations According to the Satellite Remote Sensing Data .....	60
Practical assignment No. 2: Determination of Sea Surface Temperature According to Remote Sensing Data .....	68
Practical assignment No.3: Determination of Sea Level Variability According to Satellite Altimetry Data .....	70
Practical assignment No. 4: Determination of Surface Streams Rates Components with the Use of Satellite Altimetry Data .....	75
REFERENCES .....	79

### AUTHORS:

*Ekaterina Kochetkova, Igor Kozlov:* Russian State Hydrometeorological University.

*Inga Dailidienė:* Klaipeda University.

*Konstantin Smirnov:* Saint-Petersburg State University.

*Ekaterina Kochetkova, Igor Kozlov  
Inga Dailidienė, Konstantin Smirnov*

# **REMOTE SENSING FOR OCEANOGRAPHIC APPLICATIONS**

*Textbook*

Design & desktop publishing *K.P. Eremin*

ЛР № 020309 от 30.12.96

---

Подписано в печать 27.11.2013. Формат 60x90 1/16. Гарнитура “Таймс”.

Печать цифровая. Усл. печ. л. 5,1. Тираж 100 экз. Заказ № 255/3.

РГГМУ, 195196, Санкт-Петербург, Малоохтинский пр. 98.

Отпечатано в ЦОП РГГМУ

---